

DESIGN AND OPTIMISATION OF OUTER-ROTOR
HYBRID EXCITATION FLUX SWITCHING MOTOR

MD. ZARAFI BIN AHMAD

UNIVERSITI TUN HUSSEIN ONN MALAYSIA

DESIGN AND OPTIMISATION OF OUTER-ROTOR HYBRID EXCITATION
FLUX SWITCHING MOTOR

MD. ZARAFI BIN AHMAD

A thesis submitted in
fulfillment of the requirement for the award of the
Doctor of Philosophy in Electrical Engineering

Faculty of Electrical and Electronic Engineering
Universiti Tun Hussein Onn Malaysia

SEPTEMBER 2016

*Dedicated to
my beloved father, mother, brothers and sisters
and to my beloved wife and children
and friends.
Thank you for your love, prayer, support, and patience.
I love you all deeply.*

ACKNOWLEDGEMENTS

In the name of ALLAH, the most Gracious and the Most Merciful. Alhamdulillah, all praises to Allah Almighty for His grace and His blessings given to me for the completion of my PhD studies successfully.

I also wish to express my gratitude to my supervisor, Assoc. Prof. Dr. Zainal Alam bin Haron and co-supervisor Dr. Erwan bin Sulaiman for their guidance, invaluable help, advice, and patience on my project research. Without their constructive and critical comments, continued encouragement, and good humour while facing difficulties, I could have not completed this research. I am also very grateful to them for guiding me to think critically and independently.

I acknowledge, with many thanks, to Ministry of Higher Education Malaysia (MOHE) and Universiti Tun Hussein Onn Malaysia (UTHM) for awarding me scholarship for my PhD programme. I'm much honoured to be the recipient for this award and receiving this scholarship has helped to secure my financial position during my studies and further given me the impetus to strive very hard to complete this research on time.

My sincere thanks go to Mr. Gadafi M. Romalan, for his hard work in assisting me to ensure the prototype and experiment test are implemented successfully. I also want to thank Mr. Faisal Khan, Mr. Mohd Fairoz Omar, and Mr. Mahyuzie Jenal for their contributions in sharing their knowledge and experience on electrical machine design.

Furthermore, I wish to express my sincere gratitude to my mother and father for their moral support and prayers. I would also thank to my wife for her support, endless encouragement, prayers, and love. To my children Nur Alya Md Zarafi, Muhammad Muaz Md Zarafi, and Muhammad Dariel Madinah Md Zarafi, I want to say thanks for your patience throughout my study period.

ABSTRACT

Permanent Magnet Flux Switching Motor (PMFSM) with outer-rotor configuration recently reported in the literature can potentially lead to a very compact in-wheel electric vehicle (EV) drive design and increased cabin space through the elimination of mechanical transmission gears. Nevertheless, the output torque is still insufficient to drive heavier EV especially at starting and climbing conditions. On the other hand, with the permanent magnets placed along the radial V-shaped segmented stator, the PMFSM is prone to excitation flux leakage and demagnetization, making optimisation of the rotor and stator dimensions a difficult objective to achieve, while keeping the PM volume constant. In this thesis, design and optimisation of high torque capability salient stator outer-rotor hybrid excitation flux switching motor (OR-HEFSMs) are investigated. With the additional DC field excitation coil (FEC) as a secondary flux source, the proposed motor offers advantage of flux control capability that is suitable for various operating conditions. The design restrictions and specifications of the proposed motor are kept similar as interior permanent magnet synchronous motor (IPMSM) employed in the existing hybrid electric vehicle (HEV) Toyota Lexus RX400h. The JMAG-Designer ver. 14.1 was used as 2D-finite elements analysis (FEA) solver to verify the motor's operating principle and output torque performance characteristics. The subsequent optimisation work carried out using deterministic optimisation approach (DOA) has produced a very promising 12S-14P OR-HEFSM configuration, where a maximum torque density of 12.4 Nm/kg and power density of 5.97 kW/kg have been obtained. These values are respectively 30% and 68% more than that produced by IPMSM of comparable dimensions. A reduced-scale prototype 12S-14P OR-HEFSM has also been fabricated to minimize the manufacturing cost and no-load laboratory measurements have been carried out to validate the simulation results. The results obtained show that they are in good agreement and has potential to be applied for in-wheel drive EV.

ABSTRAK

Motor Fluks Teralih Magnet Kekal (PMFSM) dengan konfigurasi pemutar di luar berpotensi digunakan untuk pemacuan kereta elektrik di dalam roda dan menyumbang kepada penyediaan ruang kabin yang lebih luas apabila tiada lagi penggunaan gear penghantaran mekanikal. Walaubagaimanapun, daya kilas yang dihasilkan masih tidak mencukupi untuk memacu kenderaan elektrik yang lebih besar terutamanya pada peringkat permulaan gerakan dan keadaan mendaki. Selain itu, dengan magnet kekal diletakkan di sepanjang jejari teras pegun berbentuk-V, ia terdedah kepada kebocoran fluks dan penyah-magnetan magnet kekal menjadikan teras pemutar dan teras pegun sukar dioptimumkan sekiranya isipadu magnet kekal adalah malar. Tesis ini membincangkan kajian dalam merekabentuk dan mengoptimumkan daya kilas motor fluks teralih pengujaan hibrid dengan pemutar di luar (OR-HEFSM). Dengan adanya tambahan gegelung medan pengujaan arus terus (AT) sebagai sumber fluks kedua, motor yang dicadangkan menjanjikan satu lagi kelebihan iaitu pengawalan fluks menjadi lebih mudah di mana ianya sangat berguna dalam pelbagai keadaan pengoperasian. Kekangan rekabentuk dan spesifikasi motor elektrik yang dicadangkan adalah berdasarkan spesifikasi motor segerak magnet kekal (IPMSM) yang digunakan di dalam kereta elektrik hibrid (HEV) Toyota Lexus RX400h. Perisian JMAG-Designer ver.14.1 telah digunakan sebagai penyelesaian analisis unsur terhingga (FEA) dua dimensi (2D) untuk mengesahkan prinsip kendalian dan prestasi daya kilas keluaran motor tersebut. Seterusnya, kajian pengoptimuman daya kilas keluaran telah dijalankan menggunakan kaedah penentuan optimasi dan berjaya menghasilkan OR-HEFSM dengan konfigurasi 12S-14P berketumpatan dayakilas sebanyak 12.4 Nm/kg dan ketumpatan kuasa sebanyak 5.93kW/kg. Nilai tersebut adalah masing-masing 30% dan 68% lebih tinggi berbanding prestasi motor IPMSM dengan diameter motor yang sama. Prototaip 12S-14P berskala kecil telah dibangunkan bagi mengurangkan kos pembuatan dan pengukuran tanpa beban telah dijalankan di makmal untuk mengesahkan keputusan yang diperolehi daripada simulasi komputer. Berdasarkan

keputusan yang diperoleh menunjukkan ciri-ciri prestasi motor tersebut adalah sejajar dengan keputusan yang diperoleh daripada simulasi dan berpotensi digunakan sebagai pemacu kereta elektrik dalam roda.

TABLE OF CONTENTS

DECLARATION	iii
DEDICATION	iv
ACKNOWLEDGEMENTS	v
ABSTRACT	vi
ABSTRAK	vii
TABLE OF CONTENTS	ix
LIST OF TABLES	xiii
LIST OF FIGURES	xiv
LIST OF SYMBOLS AND ABBREVIATIONS	xx
LIST OF APPENDICES	xxiv
CHAPTER 1 INTRODUCTION	1
1.1 Research background	1
1.2 Problem statement	2
1.3 Objectives of the study	4
1.4 Scope of works	4
1.5 Thesis outline	5
CHAPTER 2 LITERATURE REVIEW	7
2.1 Introduction	7
2.2 Overview of flux switching machines (FSMs)	7
2.3 Classification of flux switching machines (FSMs)	9

2.4	Permanent magnet flux switching machines (PMFSMs)	10
2.5	Field excitation flux switching machines (FEFSMs)	12
2.6	Hybrid excitation flux switching machines (HEFSMs)	16
2.6.1	HEFSM Topologies	16
2.6.2	Design of HEFSMs	19
2.6.3	Outer-rotor flux switching machines	20
2.6.4	Operating principle of OR-HEFSM	22
2.7	Dynamic model and equivalent circuit of OR-HEFSM	23
2.8	Cogging torque of OR-HEFSM	27
2.9	Review of optimisation methods	28
2.10	Summary	29
CHAPTER 3	RESEARCH METHODOLOGY	30
3.1	Introduction	30
3.2	Design process and setting conditions of new topology three-phase OR-HEFSM	30
3.2.1	Initial design of OR-HEFSM	31
3.2.2	JMAG-Geometry Editor	35
3.2.3	JMAG-Designer	35
3.2.4	Perform principle operation of OR-HEFSM	40
3.3	Performance investigation of OR-HEFSM at various rotor pole configurations	41
3.3.1	Torque analysis	42
3.3.2	Power analysis	44
3.3.3	Torque and power versus speed characteristics	44
3.3.4	Losses and efficiency	45
3.3.5	Torque and power densities	46
3.4	Design optimisation and mechanical analysis of OR-HEFSM	47
3.4.1	Mechanical analysis	50
3.4.2	Rotor mechanical strength analysis	50
3.4.3	Permanent magnet demagnetisation analysis	51
3.5	Reduced-scale prototype development of OR-HEFSM	51

3.5.1	Reduced-scale prototype design using SolidWorks	52
3.5.2	Experimental setting	53
3.6	Summary	54
CHAPTER 4 INITIAL DESIGN ANALYSIS OR-HEFSM AT VARIOUS ROTOR POLE CONFIGURATION		55
4.1	Introduction	55
4.2	Operating principle investigation of OR-HEFSM	56
4.2.1	Coil test analysis	56
4.2.2	Flux switching concept analysis	59
4.3	Impact of rotor pole numbers on the performances of OR-HEFSM	60
4.3.1	No-load performances OR-HEFSM at various rotor pole numbers	61
4.3.2	Load Analysis of Initial Design OR-HEFSM	67
4.4	Summary	69
CHAPTER 5 DESIGN REFINEMENT AND OPTIMISATION OF OR-HEFSM		70
5.1	Introduction	70
5.2	Results and performances of 12S-10P OR-HEFSM	70
5.2.1	Initial performances of 12S-10P OR-HEFSM	71
5.2.2	Parameter sensitivity on optimisation of 12S-10P OR-HEFSM	76
5.2.3	Final design performances of 12S-10P OR-HEFSM	81
5.3	Results and performances of 12S-14P OR-HEFSM	88
5.3.1	Initial performances of 12S-14P OR-HEFSM	89
5.3.2	Design optimisation of 12S-14P OR-HEFSM	94
5.3.3	Performance of final design 12S-14P OR-HEFSM	96
5.4	Mechanical analysis of final design OR-HEFSM based on 2D-FEA	109
5.4.1	Rotor mechanical stress prediction	110

5.4.2	Permanent magnet demagnetization investigation	111
5.5	Investigation on permanent magnet volume reduction of OR-HEFSM	112
5.6	Experimental results of reduce-scale prototype final design 12S-14P OR-HEFSM	116
5.6.1	Reduced-scale prototype 12S-14P OR-HEFSM	117
5.6.2	Measured results of reduced-scale prototype OR-HEFSM	117
5.7	Summary	124
CHAPTER 6 CONCLUSIONS AND FUTURE WORKS		125
6.1	Conclusions	125
6.2	Future works	126
6.3	Research contributions	127
REFERENCES		129
APPENDICES		142 - 153
VITA		154

LIST OF TABLES

3.1	Initial parameter of the original 12S-10P OR-HEFSM	34
3.2	Material used in the proposed ORHEFSM	38
3.3	Armature current and DC FEC current conditions	43
4.1	Flux density at various rotor pole numbers	66
4.2	Comparison of maximum output torque and power of the initial design OR-HEFSM topologies	69
5.1	Parameters comparison of initial and final design 12S-10P OR-HEFSM	82
5.2	Parameters comparison of initial and final design 12S-14P OR-HEFSM	99
5.3	Comparison of torque and power densities of OR-HEFSM and conventional IPMSM [124]	107
5.4	Output torque and power, motor losses, and efficiency at several operating points of final design OR-HEFSM	110
5.5	PM demagnetization of final design OR-HEFSM at 180°C	114
5.6	PM Demagnetization at various temperature conditions	114
5.7	Magnitude of U-phase back-emf of PM at various speed conditions	121
5.8	Magnitude of U-phase back-emf at low DC FEC current	123

LIST OF FIGURES

2.1	Rotor position of flux switching inductor alternator, (a) $\theta = 0$ degree (b) $\theta = 90$ degrees [30]	8
2.2	Various categories of electrical machines.	9
2.3	Topologies of PMFSMs. (a) 12S-10P PMFSM with all poles wound, (b) PMFSM with alternate poles wound, (c) E-core PMFSM, (d) C-core PMFSM, (e) Multi-tooth PMFSM, (f) Segmental rotor PMFSM with all poles wound	11
2.4	Example of FEFSMs (a) 1-phase 4S-2P FEFSM (b) 1-phase 8S-4P FEFSM (c) 3-phase 24S-10P FEFSM (d) 3-phase 12S-8P segmental rotor FEFSM	14
2.5	Three-phase salient rotor WFFSM (a) 12S-10P with overlapped windings, (b) 12S-10P with non- overlapped windings, (c) 6S-10P non-overlapped windings	15
2.6	Example of HEFSMs (a) 6S-4P HEFSM (b) 12S-10P Inner FEC HEFSM (c) 12S-10P Outer FEC HEFSM (d) 12S-10P E-core HEFSM (e) Radial FEC HEFSM	18
2.7	12S-22P outer-rotor PMFSM [23].	22
2.8	Principle operation of OR-HEFSM (a) $\theta_e = 0^\circ$ (b) $\theta_e =$ 180° more excitation, (c) $\theta_e = 0^\circ$ (b) $\theta_e = 180^\circ$ less excitation.	23
2.9	d - q axis equivalent circuits of HEFSM.	25
3.1	General research flow implementation	31
3.2	Cross sectional view of initial design 12S-10P OR- HEFSM	32

3.3	Design parameters of D_1 to D_{10} of 12-10P OR-HEFSM	34
3.4	Drawing, setting, and operating principle analysis using JMAG-Geometry Editor and JMAG-Designer	36
3.5	Region radial pattern, (a) rotor (b) stator	37
3.6	12S-10P OR-HEFSM drawn in Geometry Editor	37
3.7	Winding configuration of 12S-10P OR-HEFSM	38
3.8	Circuit construction (a) Armature coil circuit (b) FEC circuit (c) Three-phase star-connected circuit and current supply unit	39
3.9	Work flow of armature coil test analysis	41
3.10	Various pole numbers of OR-HEFSM	42
3.11	Workflow of no load and with load analysis	43
3.12	Typical torque and power versus speed characteristic of synchronous motor	45
3.13	Estimated coil end volume of OR-HEFSM	47
3.14	Defined optimisation parameters L_1 to L_{10}	48
3.15	Deterministic optimisation approach	49
3.16	Rotating rotor at constant speed	50
3.17	BH curve of NEOMAX-35AH	52
3.18	Block diagram of experimental setup	53
4.1	Initial PM and coil winding polarity of OR-HEFSM	56
4.2	Magnetic flux observed in armature coil; (a) coil C1, C4, C7, and C10 (b) coil C2, C5, C8, and C11 (c) coil C3, C6, C9, and C12	57
4.3	Three-phase armature coil arrangement of OR-HEFSM	58
4.4	Three-phase magnetic flux of 12S-10P OR-HEFSM	59
4.5	Flux distribution at several rotor position (a) $\theta = 0^\circ$, (b) $\theta = 9^\circ$, (c) $\theta = 18^\circ$, and (d) $\theta = 27^\circ$	60
4.6	U-phase magnetic flux linkage at various rotor pole configurations (a) PM flux (b) DC FEC flux	61
4.7	Back-emf at 3,000r/min	62

4.8	Cogging torque of initial design OR-HEFSM at various rotor pole numbers	63
4.9	Magnitude of peak-to-peak cogging torque of the initial design OR-HEFSM	63
4.10	Flux line and three-phase flux linkage of various rotor pole numbers of the initial design OR-HEFSM (a) 12S-10P (b) 12S-14P, and (c) 12S-16P	64
4.11	Flux line and three-phase flux linkage of various rotor pole numbers of the initial design OR-HEFSM (a) 12S-20P (b) 12S-22P (c) 12S-26P	65
4.12	Flux strengthening at various DC FEC current densities	67
4.13	Torque at various DC FEC current densities of initial design OR-HEFSM	68
4.14	Power at various DC FEC current densities of initial design OR-HEFSM	68
5.1	Main machine dimension of the proposed 12S-10P OR-HEFSM	71
5.2	U-phase flux linkage of initial design OR-HEFSM	72
5.3	Flux path of PM only of 12S-10P OR-HEFSM (a) 0°/36° rotor position, (b) 9° rotor position, (c) 18° rotor position, (d) 27° rotor position	73
5.4	Magnetic flux distribution (a) $J_e = 10\text{A/mm}^2$, (b) $J_e = 20\text{A/mm}^2$, and (c) $J_e = 30\text{A/mm}^2$	74
5.5	Back-emf at 3,000r/min of initial design 12S-10P OR-HEFSM	75
5.6	Initial torque characteristics at various current density conditions	76
5.7	Torque versus inner rotor radius, L_1	77
5.8	Torque versus inner rotor radius, L_2 at various L_3	77
5.9	Torque versus PM width, L_5 at various L_4	78
5.10	Torque performance at various L_6 and L_7	79
5.11	Torque and power at various L_8 and L_9 of armature coil slot	79

5.12	Torque and power performance of 12S-10P OR-HEFSM at several optimisation cycles	80
5.13	Final design 12S-10P OR-HEFSM	81
5.14	Comparison of U-phase flux linkage of 12S-10P OR-HEFSM (a) Initial design (b) Final design	83
5.15	Structure comparison of 12S-10P OR-HEFSM (a) Initial design (b) Final design	84
5.16	PM flux path of 12S-10P OR-HEFSM (a) Initial design (b) Final design	84
5.17	Back-emf of 12S-10P OR-HEFSM at speed 3000r/min	85
5.18	Cogging torque of 12S-10P OR-HEFSM	86
5.19	Torque comparison of 12S-10P OR-HEFSM	86
5.20	The instantaneous torque of 12S-10P OR-HEFSM	87
5.21	Torque characteristics of final design 12S-10P OR-HEFSM at various conditions of J_e and J_a	87
5.22	Initial designed structure of 12S-14P OR-HEFSM	89
5.23	U-phase magnetic flux of PM, DC FEC, and armature coil	90
5.24	U-phase flux linkage at various DC FEC current densities	90
5.25	Cogging torque of initial design 12S-14P OR-HEFSM	91
5.26	Back-emf of initial design 12S-14P OR-HEFSM at 3000 r/min	92
5.27	Magnetic flux distribution of initial design 12S-14P OR-HEFSM	93
5.28	Torque characteristic at various current densities	94
5.29	Torque and power performance at different armature coil turns	96
5.30	Final design OR-HEFSM parameters	97
5.31	Magnetic flux distribution at high current density; (a) Initial design (b) Final design	98

5.32	Flux path of final design 12S-14P OR-HEFSM (a) PM only (b) PM and maximum J_e	100
5.33	U-phase back-emf of initial and final design OR- HEFSM at 3000r/min	100
5.34	Harmonics content of 12S-14P OR-HEFSM	101
5.35	Cogging torque of OR-HEFSM	102
5.36	Toque performance at various current density conditions	102
5.37	Torque and power versus armature current phase angle (a) Torque (b) Power	104
5.38	Torque versus speed at various J_a and angle of armature current, I_a	105
5.39	Torque versus speed characteristics	105
5.41	Power versus speed characteristics	106
5.40	Instantaneous torque of initial and final design 12S- 14P OR-HEFSM	106
5.42	Distribution of iron and copper loss final design 12S- 14P OR-HEFSM	109
5.43	Efficiency of final design OR-HEFSM	109
5.44	Principal stress distribution of 12S-14P OR-HEFSM (a) Initial design. (b) Final design	111
5.45	PM demagnetization of final design OR-HEFSM at 180°C	113
5.46	Torque versus PM weight	115
5.47	Torque versus number of armature coil turns at various PM weight	115
5.48	Torque of various PM weight at various angle of armature current	116
5.49	12S-14P OR-HEFSM with 800g PM weight	117
5.50	Prototype machine designed using SolidWorks (a) Stator with windings (b) Rotor coupled with shaft and holder (c) Shaft (d) Casing (e) Exploded view	118
5.51	Reduced-scale prototype of 12S-14P OR-HEFSM (a) Stator with PM (b) Stator with windings (c) Rotor	

	core (d) Rotor attached to holder and shaft (e) Overall machine and casing	119
5.52	Experimental workbench setup	120
5.53	Three-phase back-emf at 1200 rpm	120
5.54	U-phase back-emf of PM only final design 12S-14P OR-HEFSM	121
5.55	Comparison of maximum back-emf of final design reduced-scale 12S-14P OR-HEFSM	122
5.56	U-phase back-emf of PM and FEC final design reduced-scale 12S-14P OR-HEFSM	122
5.57	Average torque versus FEC currents	123

LIST OF SYMBOLS AND ABBREVIATIONS

ψ_e	-	Flux linkage due to excitation components
ϕ_m	-	PM flux linkage
ϕ_e	-	Field excitation flux linkage
α_a	-	Filling factor of armature coil
α_{cog}	-	Electrical angle of rotation
α_e	-	Filling factor of excitation coil
α_f	-	Filling factor
η	-	Efficiency
θ	-	Electrical angular position of rotor
ω_r	-	Rotational speed
ρ	-	Copper resistivity
A_n	-	Cross sectional area of PM
B_n	-	Magnetic flux density
D	-	Damping factor
D_y	-	Dysprosium
F_c	-	Force in cylindrical body
f_e	-	Electrical frequency
f_m	-	Mechanical rotation frequency
H	-	Height of coil slot
I_a	-	Armature coil current
I_e	-	Field excitation coil current
i_d	-	d-axis current
i_q	-	q-axis current

J_a	-	Armature current density
J_e	-	Field current density
k	-	Natural number
kW	-	Kilowatt
ℓ	-	Stack length
L	-	Coil length
$L_{a,e}$	-	Stack length of machine
L_{a-end}	-	Estimated average length of armature end coil
L_d	-	d-axis inductance
L_{a-end}	-	Estimated average length of field excitation end coil
L_f	-	Total series inductance of field coil
L_q	-	q-axis inductance
N	-	Number of turns
n	-	Number of elements
N_a	-	Number of turns of armature coil
N_{a-slot}	-	Number of slots of armature coil
N_{cog}	-	Number of cycles of cogging torque
N_d	-	Neodymium
N_e	-	Number of turns of field excitation coil
N_{e-slot}	-	Number of slots of field excitation coil
N_p	-	Number of periods of cogging torque
N_r	-	Number of rotor poles
N_s	-	Number of stator slots
p	-	Pole pairs number
P_a	-	Armature coil loss
P_c	-	Copper loss
P_i	-	Iron loss
P_{max}	-	Maximum power
P_o	-	Output power
q	-	Number of phases
R_a	-	per-phase armature coil resistance
R_c	-	iron core resistance

R_f	-	Total series resistance of field coil
R_{in}	-	Inner radius of coil end
R_{out}	-	Outer radius of coil end
S_a	-	Armature coil slot area
S_e	-	Field excitation coil slot area
T_e	-	Electromagnetic torque
T_L	-	Load torque
T_{max}	-	Maximum torque
V_1	-	Volume of coil slot
V_2	-	Volume of coil end
V_{total}	-	Total volume of coil
W	-	Width of coil slot
$x_{d,q}$	-	Components in d-q axis
$x_{u,v,w}$	-	Components of U, V, and W phase
AC	-	Alternating current
CNC	-	Computer numerical control
CO ₂	-	Carbon dioxide
DC	-	Direct current
DOA	-	Deterministic optimisation approach
EV	-	Electric vehicle
FE	-	Field excitation
FEA	-	Finite Element Analysis
FEC	-	Field Excitation Coil
FEFSM	-	Field excitation flux switching machine
FSM	-	Flux switching motor
HCF	-	Highest common factor
HE	-	Hybrid Excitation
HEFSM	-	Hybrid excitation flux switching machine
HEV	-	Hybrid Electric Vehicle
IPMSM	-	Interior permanent magnet synchronous motor
NdFeB	-	Neodymium magnet
OR-HEFSM	-	Outer-rotor hybrid excitation flux switching machine

PM	-	Permanent magnet
PMFSM	-	Permanent magnet flux switching machine
PMSM	-	Permanent magnet synchronous machine
SRM	-	Switched-reluctance machine
WFFSM	-	Wound Field Flux Switching Machine
WFSM	-	Wound Field Synchronous Machine

LIST OF APPENDICES

APPENDIX	TITLE	PAGE
A	List of Publications	142
B	List of Awards	145
C	Table C: Design restrictions, specifications, and target performances of the proposed OR-HEFSM for in-wheel drive EV applications	147
D	Table D: Specifications of reduced-scale prototype OR-HEFSM	148
E	Non-Oriented Electrical Steel Sheets	149
F	F1. Technical drawing of the rotor OR-HEFSM	151
	F2. Technical drawing of the stator OR-HEFSM	152
	F3. Technical drawing of the shaft OR-HEFSM	153

CHAPTER 1

INTRODUCTION

1.1 Research background

Transportation sector is among the major contributors of carbon dioxide (CO₂) emissions globally, which represents about 23% of fossil fuel combustion by-products [1]. Current mainstream opinion is that the electric vehicle (EV) is the most promising solution for reducing carbon dioxide (CO₂) emissions from the transportation sector. In addition, it is projected that the depleting petroleum resources will lead the world to an energy crisis in the next few decades unless viable alternative energy sources are found [2]–[5]. These two issues are the main problems pressing the automotive industry, propelling their research activities to come up with a green and most fuel-efficient vehicle that meets zero emission vehicles as early as possible.

In conventional centralised drive of EVs, mechanical components such as transmission gear, differential gear, and belting take up precious cabin space, increasing the overall weight of EV and energy losses due to friction. The emergence of direct drive in-wheel motor has brought about a great opportunity to EV car manufacturers to eliminate the mechanical transmission components in conventional centralised drive [6],[7]. Furthermore, the greater cabin space availability can be advantageously used for series batteries installation and contributes to a longer driving range per-charge.

Electric motor is the most essential part of an EV motor drive system. Typical design requirements for an EV motor drive are: (i) high torque and power densities;

(ii) high torque at low speed for starting and climbing; (iii) wide speed range at constant torque and constant power; (iv) fast torque response for braking; (v) low cogging torque for refined drivability; (vi) high efficiency; and (vii) reasonable cost [7]–[10].

In recent years, research and development of flux switching machines (FSMs) have become increasingly popular due to their advantages of high torque density, robust rotor structure, less weight, and easy cooling system management [11],[12]. With a salient rotor structure and all excitation components (either PM or excitation coil) and armature coil located in the stator, the machine accrues the combined advantages of the permanent magnet synchronous machine (PMSM) and switched-reluctance machine (SRM).

For over a decade, research and development on PMFSM has growing rapidly and many topologies have been introduced and investigated. Nevertheless, with the continuing increase of the price of rare-earth magnets [13], researchers are now focusing on high torque machine topologies that use minimum or no permanent magnets [14]–[16]. Due to that reason, research and development of HEFSMs are getting attractive not only to save the material cost but also to improve the flux weakening capability and efficiency. Moreover, the HEFSM topologies allow safe operation at high speeds while the PM helps to increase the efficiency of the motor [17],[18].

More recently, in-wheel drive motors for EVs has generated a great deal of interest due to the elimination of mechanical transmission and differential gears and their associated mechanical parts. Nevertheless, selection of a suitable traction motor for in-wheel drive is very important and requires special attention. A number of researchers [7], [19]–[23] are of the view that an in-wheel outer-rotor motor have very significant advantages over the conventional inner-rotor configuration due to the capability to deliver higher torque density and compactness.

1.2 Problem statement

In-wheel direct drive is becoming more popular due to the elimination of the conventional transmission gearing system and the resulting increase in cabin space can be used to put in more battery. Thus, the in-wheel direct drive not only provides

optimal torque directly to the wheel, but it also contributes to a lighter vehicle and a longer driving range per-charge. In terms of torque and power densities, and the greater reliability of in-wheel drive motors, outer-rotor machine configuration is the best candidate compared with the conventional inner-rotor motor [7]. Previously, research on PM-rotor PMSMs have dominated the outer-rotor in-wheel drive application due to their high torque and power densities. Nevertheless, due to the un-robust rotor structure and the difficulty to remove heat from the PM-rotor, the outer-rotor PMFSM has been introduced only for light EVs application [23]. The machine comprises of a passive and robust salient-pole rotor, and all active components of armature windings and permanent magnets are accommodated at the stator. While the PMFSM has managed to achieve a better output torque capability, but it is still not sufficient to drive heavier EV. Besides that, the constant flux of the permanent magnet exposes it to demagnetization and uncontrollability problems when the machine operates at high temperature and flux weakening mode, respectively [24]. Moreover, the ever increasing price of rare-earth magnet used in PMFSM is also another constraint limiting further development of the machine [14]. Concomitantly, the V-shape segmented stator structure makes manual assembly of the machine very difficult and optimisation of its performance a challenging task. Hence, the aforementioned problems has attracted a lot of research and development efforts in alternative machine topologies for solution. There are numerous papers on FSM have been published and appears to be an absence of any research effort on the development of the outer-rotor HEFSM (OR-HEFSM) for in-wheel drive application. In view of this perceived lack of interest by other researchers in the use of OR-HEFSM for in-wheel direct drive, this research proposes a new OR-HEFSM with a salient stator topology that potentially can give a much higher torque and power densities compared to IPMSM employed in Toyota Lexus RX400h [25]. In this work it is proposed to use an additional DC FEC as a secondary excitation flux source to improve flux control capability, diminish PM demagnetization and save PM material cost, and a salient stator geometry to help simplify the fabrication process. It is expected that these improvements will lead to a more robust rotor structure and higher output torque and power densities that makes the machine particularly suitable for in-wheel direct drive EV.

1.3 Objectives of the study

The main objective of this research is to develop a new OR-HEFSM topology with inherently high torque and power densities for in-wheel direct drive EV application. In achieving the main objective, there are some specific objectives that have to be fulfilled, which are:

- (i) To propose a salient stator OR-HEFSM topology and investigate its operating principle and output performances at various current densities.
- (ii) To optimise the proposed motor to examine the optimal output torque capability.
- (iii) To validate the simulation results experimentally based on reduced-scale prototype of the proposed motor.

1.4 Scope of works

Computer simulation studies were carried out to design the proposed structure and investigate the operating characteristic of OR-HEFSM topologies. In particular, the study investigates the initial performance of flux strengthening, flux distribution, back-emf, cogging torque, and maximum torque and power. The commercial JMAG-Designer ver.14.1, released by JSOL Corporation, Japan was used as 2D-finite element analysis (FEA) solver. The design restrictions, target specifications, and parameters of the proposed OR-HEFSM are based on the conventional interior PMSM (IPMSM) used in existing hybrid electric vehicle (HEV), Toyota RX400h. The electrical restrictions related with the inverter such as maximum 650V DC bus voltage and maximum 360 A(rms) inverter current were set similar as in the IPMSM used in the existing Toyota RX400h [25]. Details of the motor specifications are given in Appendix C.

In simulation works, the highest maximum current density of $30\text{A}/\text{mm}^2$ that can be handled by the coils was assigned. Then, the machines' back electromagnetic-force (back-emf), cogging torque, flux strengthening, torque speed characteristics, average torque, mechanical effects, machine losses and efficiency were analyzed using 2D-FEA. Only the 12 stator-slot topologies were investigated, with the number of rotor

poles limited to 10, 14, 16, 20, 22, and 26 teeth. Optimisation works using the deterministic optimisation approach (DOA) were then carried out on 12S-10P and 12S-14P topologies to determine which one gave the maximum output torque.

A reduced-scale model of the actual motor was fabricated and its performance characteristics measured experimentally in the laboratory. The results obtained were compared with the computer simulation results to verify motor's operating principle and validate the armature coil phase sequence and back-emf waveforms. Due to the constraint of DC power supply with purely DC signal, the FEC is only fed by low current up to 8A. Whilst, the output signals are observed by 1 kV 5 Mhz power analyzer. Details on the dimension of the reduced-scale prototype are given in Appendix D.

1.5 Thesis outline

The thesis is organized as follows:

Chapter 2 reviews the historical development of FSMs from the first prototype machine to the multifarious present-day designs. Several FSM and HEFSM topologies are briefly reviewed and their pros and cons discussed. The chapter ends with short introduction on the principle operation of the HEFSM, the related mathematical model and equivalent circuit, and the advantages and disadvantages of outer-rotor configuration for in-wheel drive application.

Chapter 3 describes the computer design of the proposed OR-HEFSM implemented using JMAG-Designer software. The design stage is divided into four phases, namely, (1) Computer validation of the machine's operating principle, (2) Performance analysis, (3) Optimisation of the machine's mechanical dimension, and (4) A reduced scale prototype fabrication and testing.

Chapter 4 validates the operating principle of the proposed OR-HEFSM by performing a coil test to analyse its flux linkage. Initial performances of the proposed machine with various rotor pole configurations are shown in this chapter. Then, no-load and load analyses are presented to identify the best rotor pole configuration that gives the highest torque value and power densities.

Chapter 5 gives the detailed results obtained from optimisation of the 12S-10P and 12S-14P OR-HEFSMs utilizing the deterministic optimisation approach (DOA), viz. the machine's flux linkage, back-emf, cogging torque, flux strengthening, maximum torque and power, torque and power densities, torque/power-speed characteristic and efficiency. The mechanical analyses undertaken, viz. PM demagnetization and rotor stress that helped identify the optimum torque are also discussed here. The chapter ends with a discussion on PM volume reduction of 12S-14P and the experimental results obtained from measurement carried out on the reduced scale prototype 12S-14P OR-HEFSM.

Chapter 6 concludes this research study by giving a summary of the main results and suggesting directions for future research.

CHAPTER 2

LITERATURE REVIEW

2.1 Introduction

This chapter describes the overview of FSM topologies from the first prototype machine to the multifarious present-day designs. Three classes of FSM which are permanent magnet flux switching machines (PMFSMs), field excitation flux switching machines (FEFSMs), and hybrid excitation flux switching machines (HEFSMs) together with their several developed topologies are elaborated. Their pros and cons in terms of developed structure are also explained in brief as a comparison. Furthermore, the outer-rotor FSM configuration and its operating principle is described in details. The related mathematical models and equivalent circuits together with the cogging torque equations are also discussed. Finally, the overview of several optimisation methods typically used in design of electrical machines are briefly explained at the end of this chapter.

2.2 Overview of flux switching machines (FSMs)

Brushless PM machines are usually designed with magnets in the rotor and henceforth called by rotor-PM machines. However, recently a number of research works have been undertaken on electric brushless machines in which the magnets are mounted on the stator. These so-called stator-PM machines have two advantages which are the stator temperature rise can easily be controlled and the PM is not subjected to the

centrifugal forces of the rotating rotor [26]–[28]. Among the stator-PM machines that have recently gained significant attention of machine designers is the flux switching machine (FSM). The motor has a double salient topology and its rotor position determines the excitation flux path on the stator, this leads to a very efficient flux coupling with the stator coil.

The single-phase FSM first proposed by A. E. Laws in 1952 was a motor and had four stator slots and four rotor poles [29]. The first generator application of the FSM concept was a single-phase machine having four stator slots, and four or six rotor poles which found immediate application in aircraft [30]. The basic principle of FSM elucidated in [30] can be easily understood by referring to the rotor position of simple alternator mechanism shown in Figures 2.1(a) and (b). It consists of a pair of stator windings, two sets of laminated yolks, and a pair of PMs, which are located on the stator, while the rotor only has two salient poles attached to the shaft. As can be seen from Figure 2.1(a), the magnetic flux emanates from the north pole of the PM on the left side of the machine and flows in a clockwise direction in the stator, making a complete flux cycle. When the rotor position is moved anti-clockwise by one-half electrical cycle, as shown in Figure 2.1(b), the same flux now reverses its direction of flow through the adjacent stator tooth.

Polyphase motor using the FSM concept was first reported in 1997 by E. Hoang et al. [31]. Since then, many new and novel FSM topologies have been developed for

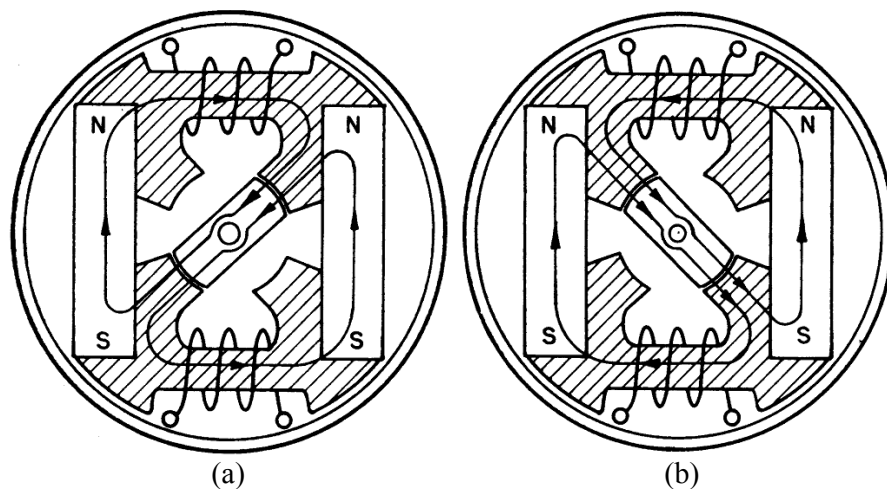


Figure 2.1: Rotor position of flux switching inductor alternator, (a) $\theta = 0$ degree
(b) $\theta = 90$ degrees [30]

various applications, ranging from low-cost domestic appliances to heavy-duty applications such in automotive drive system, wind power generators and aerospace industries [12],[32],[33]–[38].

2.3 Classification of flux switching machines (FSMs)

FSMs can broadly be classified into three groups, namely permanent magnet (PM) FSMs, hybrid excitation (HE) FSMs, and field excitation (FE) FSMs. PMFSMs and FEFSMs having a single excitation flux source each, which comes from PM and FE coil, respectively. HEFSMs, on the other hand, have two magnetic flux sources, one a PM and the other a FEC [32],[39]. The three sub-categories of FSM AC machines can be seen from the tree diagram shown in Figure 2.2.

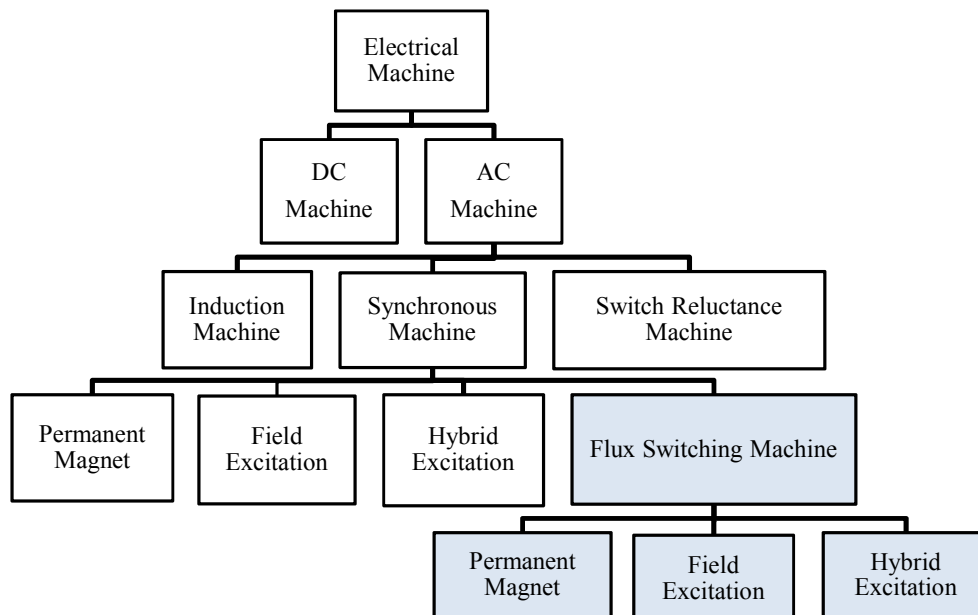


Figure 2.2: Various categories of electrical machines.

2.4 Permanent magnet flux switching machines (PMFMSs)

A working prototype three-phase PMFSM was first demonstrated by E. Hoang in 1997 [31]. Since then, many new designs have been proposed for various applications to achieve better performance either in terms of output torque, power, maximum speed, or machine efficiency. Nevertheless, this machine utilizes a unipolar flux in the stator, thus limiting the maximum torque that can be achieved [40]. The bipolar flux FSM proposed in [41] overcomes the limited torque capability of FSMs by enabling a greater flux density to be created in the air gap, and hence doubling the maximum torque that can be produced.

The list below gives the different types of PMFSM that have been developed for different applications.

- (i) Single-phase to multi-phase PMFSM [31],[42]–[44].
- (ii) Rotary and linear PMFMSs [45]–[50].
- (iii) Radial, axial-field, and transverse flux PMFMSs [35], [51], [52].
- (iv) Fault-tolerant PMFMSs [50],[53].
- (v) Outer-rotor PMFSM [23].
- (vi) E-core and C-core PMFMSs [54],[55]
- (vii) Segmental rotor PMFSM [56]
- (viii) Single-tooth or multi-tooth rotor pole of PMFMSs [57],[58],[59]

Six different three-phase PMFSM topologies are illustrated in Figure 2.3. Figure 2.3(a) shows a typical three-phase 12S-10P PMFSM, where the salient pole stator core consists of modular U-shaped laminated segments, with the armature coil wound in a concentrated arrangement. The PM, on the other hand, is accommodated in between each U-shaped section of the stator core and is put opposite of each other [31]. The salient pole rotor geometry is similar to that of SRMs, making PMFSM more robust and suitable for high-speed applications. However, in contrast with the conventional IPMSM, the coil slot area is slightly reduced when the magnets are moved from the rotor to the stator. The reduced slot area reduces the number of coil windings that can be used and hence lowers the output torque of the machine. However, the temperature rise in the magnet now becomes much easier to control by installing a cooling system. In addition, placing the PM on the stator gives the machine a high flux weakening capability while the higher per unit winding inductance obtained

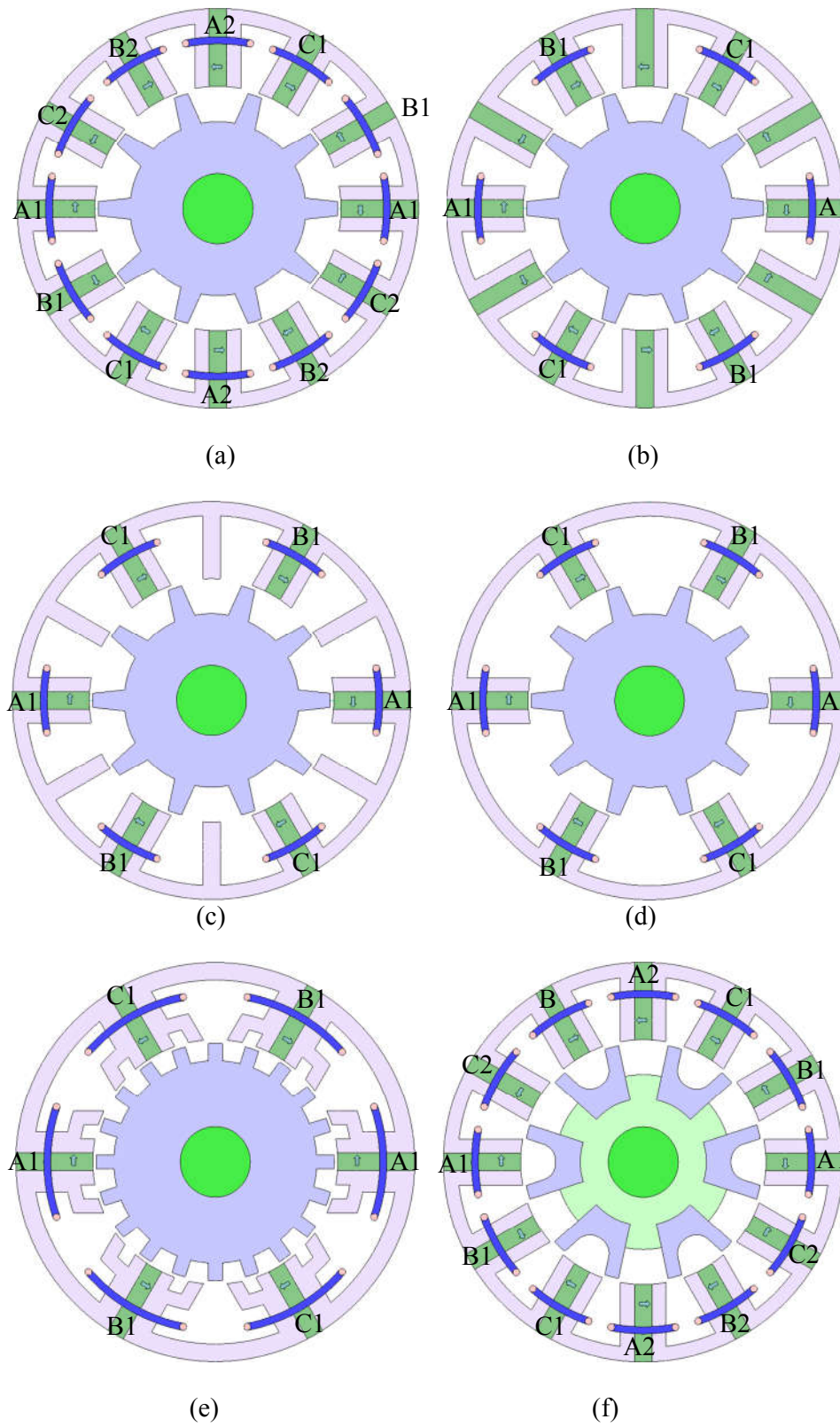


Figure 2.3: Topologies of PMFSMs. (a) 12S-10P PMFSM with all poles wound, (b) PMFSM with alternate poles wound, (c) E-core PMFSM, (d) C-core PMFSM, (e) Multi-tooth PMFSM, (f) Segmental rotor PMFSM with all poles wound

makes the machine capable of providing constant power operation over a wide speed range [60],[61].

R. L. Owen et al. has found that by removing armature windings of alternate stator poles the fault tolerant capability of the machine is improved [53]. In the FSM shown in Figure 2.3(b) armature windings A2, B2 and C2 have been removed, leaving the machine with only six armature windings. Thus, while the PM volume has not been reduced the fewer armature coils used results in less copper loss. Unfortunately, the topologies shown in Figures 2.3(a) and (b) use very high PM volumes that will increase the manufacturing cost. Hence, the PMs at the stator pole without the armature winding are removed and simple stator tooth is redesigned to form E-core 12S-10P PMFSM, as shown in Figure 2.3(c) [54],[62]. From this figure, half of the PM volume in Figure 2.3(b) is removed, and the stator core is combined together to form E-Core stator. Further enhancement on the E-core structure in which the middle E-stator teeth is removed to enlarge the slot area, and successively a new C-core 6S-10P PMFSM is established as exemplified in Figure 2.3(d) [63].

Recently, PMFSM with multi-tooth stator has been proposed as in [58] to improve the air-gap flux density and to reduce PM usage. As can be seen in Figure 2.3(e), the end of the stator tooth has a bifurcated pole to allow the flux to flow easily through all rotor teeth. However, the disadvantage of this topology is the need to have a high number of rotor poles, which consequently requires an inverter supply frequency twice that used in the machine shown in Figure 2.3(d). Akim Zulu et al. has proposed a three-phase 12S-10P PMFSM topology with segmental rotor to reduce flux leakage and shorten the flux path [56]. Nevertheless, the segmental nature of the rotor makes it mechanically less robust and hence unsuitable for high-speed applications.

2.5 Field excitation flux switching machines (FEFSMs)

PM-excited FSMs characteristically use a high volume of PM, whose most important ingredients are the rare-earth elements Neodymium (N_d) and Dysprosium (D_y). Unfortunately, the increasing annual consumption of these elements has forced their prices to escalate steeply due to supply shortages [13]. To circumvent problems associated with the ever increasing price of these elements, research and development effort on FSMs have recently moved towards topologies that use little or no PM at all.

One topology that has been actively researched recently is the FSM with DC FECs. This FEFSM is a form of salient-rotor reluctance machine which uses both the principles of the inductor generator and the SRMs for its operation [64],[65]. By changing the rotor position the flux linking with the armature winding is automatically switched to the alternate path to continue providing the attractive force to turn the rotor. This approach leads to a much simplified design, lower manufacturing cost, and zero PM usage. At the same time the FEFSM topology provides variable flux control capability, a feature that is very important in various operating conditions.

To date, many different FEFSM topologies have been investigated [66]–[73]; one early example is the single-phase 4S-2P FEFSM with toothed-rotor, shown in Figure 2.4(a) [67]. In the single-phase 4S-2P FEFSM shown, two pairs of armature coil and FEC windings are located at the stator in an overlapped configuration; leading to a very simple design and requiring only a simple electronic controller. Figure 2.4(b) shows another example of single-phase FEFSM, this time a machine with 8S-4P topology [68]. Here the FEC windings are accommodated in four slots to produce 2 pairs of alternate north-south magnetic poles, while the another four slots form two pairs of armature winding; with the armature coils and FEC windings overlapping each other. While the machine produces a higher output torque figure and efficiency value, the single-phase machine is exposed with problems such as low starting torque, large torque ripple, and a fixed direction of rotation. Furthermore, the overlapping of the armature coil and FEC results in longer end windings, thus increasing the copper loss.

The main drawbacks of the single-phase FEFSMs outlined above are largely eliminated in the three-phase 12S-10P FEFSM shown in Figure 2.4(c), where the PMs in the 12S-10P PMFSM are replaced with FEC windings wound in the outer layer [69]. The shorter end windings result in much smaller stator copper losses and a higher starting torque due to increased flux linkage. Furthermore, the greater number of poles present in the three-phase 12S-10P FEFSM help reduce the torque ripple and also simplifies control of the direction of rotation. Nevertheless, the output torque of the machine is somewhat lowered due to the presence of the unused stator teeth and isolated FECs, as indicated by the circles shown in Figure 2.4(c).

Significant improvement in the output torque is obtained by applying segmental rotor design to the three-phase 12S-8P FEFSM, and choosing a concentrated winding arrangement over a distributed one. The use of a concentrated winding arrangement helps increase the flux linkage between the rotor and the stator, and at the

same time helps reduce the copper losses, as shown in Figure 2.4(d) [70]. As a consequent, the overall efficiency of the machine is improved. Nevertheless, the segmented FEFSM rotor is less robust than a salient rotor, making it inappropriate for use in machines operating at high-speeds. Currently, research are actively carried out to solve this issue.

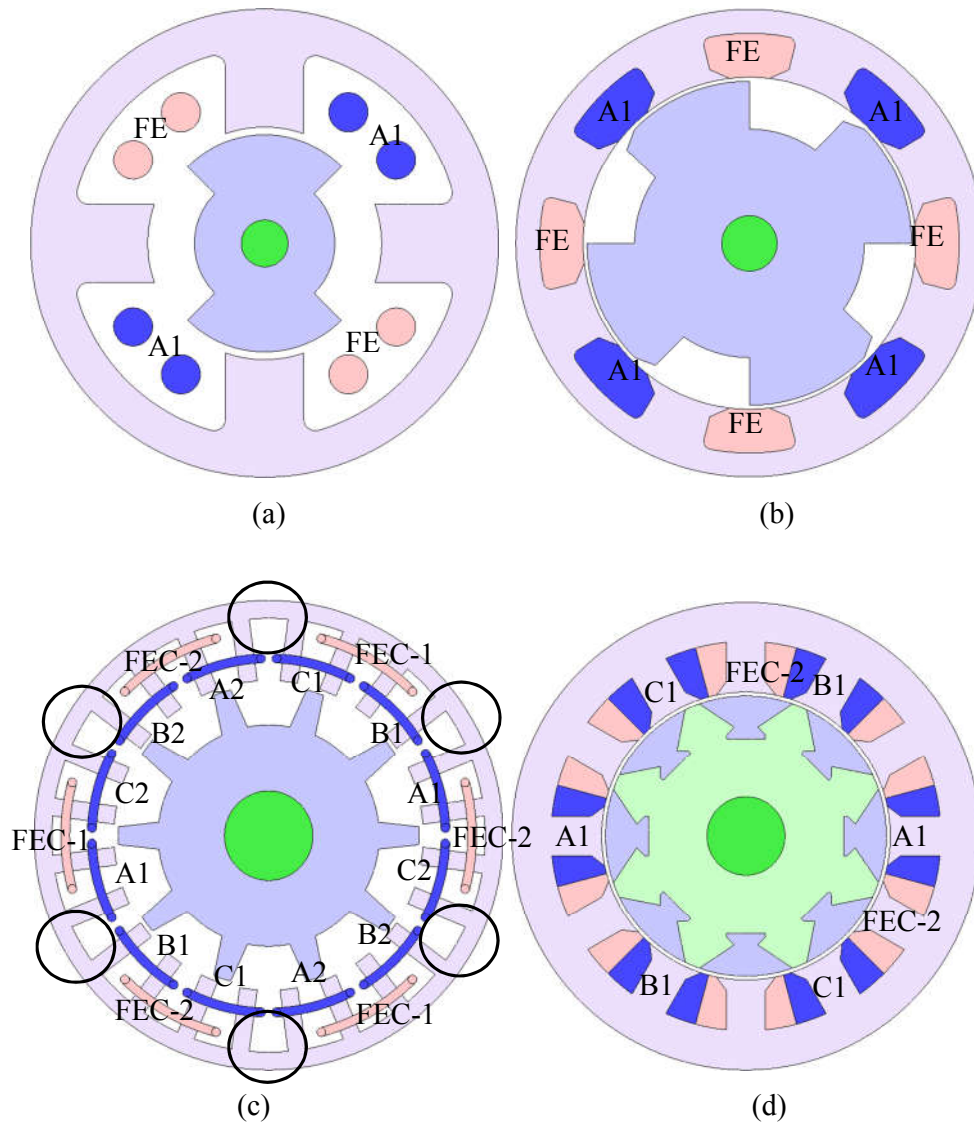


Figure 2.4: Example of FEFSMs (a) 1-phase 4S-2P FEFSM (b) 1-phase 8S-4P FEFSM (c) 3-phase 24S-10P FEFSM (d) 3-phase 12S-8P segmental rotor FEFSM

Recently, a three-phase 12S-10P wound field flux switching machine (WFFSM) with salient rotor has been proposed for hybrid EV (HEV) application [71]. The proposed machine architecture is illustrated in Figure 2.5(a). Tests carried out on the prototype machine fabricated confirmed robustness of the single-piece rotor design and measurements carried out on the machine indicated that a higher torque density can be achieved compared to conventional FEFSMs of similar dimensions. Nevertheless, the overlapping armature coil and FEC windings results in a less efficient machine due to high copper losses occurring in the coils. More recently, a

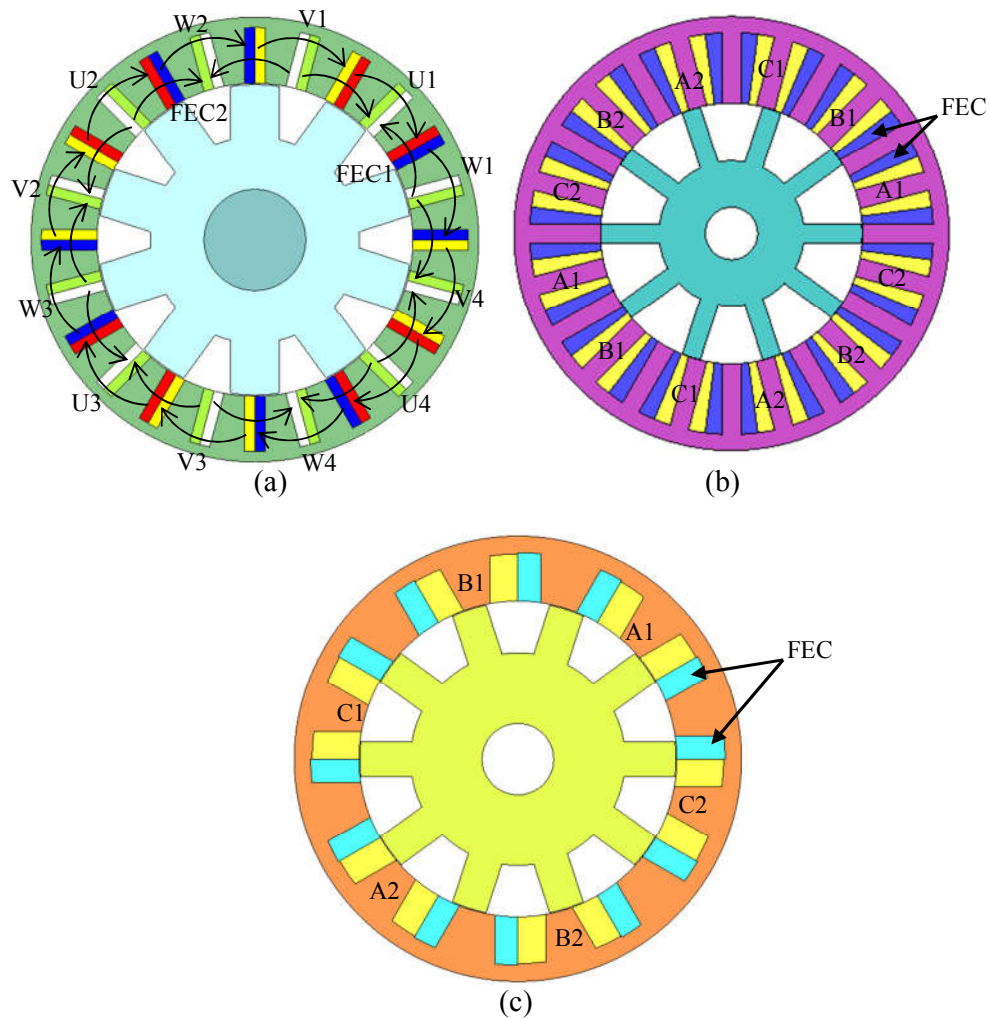


Figure 2.5: Three-phase salient rotor WFFSM (a) 12S-10P with overlapped windings, (b) 12S-10P with non-overlapped windings, (c) 6S-10P non-overlapped windings

12S-10P WFFSM has been developed that combines the advantages of FEFSM with segmental rotor shown in Figure 2.4(d) and WFFSM shown in Figure 2.5(a). The resulting machine architecture is shown in Figure 2.5(b) [72]. However, this 12S-10P WFFSM proposed by F. Khan gave a low output torque due to the use of too many stator slots. Subsequent torque improvement was achieved by reducing the number of stator slots from 12 to 6 (see Figure 2.4(d)) and optimizing the stator and rotor dimensions [73].

2.6 Hybrid excitation flux switching machines (HEFSMs)

The vastly superior torque performance at low speeds coupled with a high power output over a wide speed range compared to conventional IPMSM has made the PMFSM very suitable for EV propulsion system. On the other hand, the ever increasing price of rare-earth magnets is making PM-based FSM machines economically uncompetitive compared to FEFSMs and HEFSMs. In addition, PMFSMs are difficult to operate beyond their base speeds in the flux weakening region, which requires control of the armature winding current. Operating the PMFSM beyond its base speed requires a higher armature winding current, which results in a higher copper loss, reduction in operating efficiency and power capability, and also possible irreversible demagnetization of the PMs. On the other hand, FEFSMs have totally resolved the issue of high PM price by totally eliminating the need for PM in conventional PMFSMs. Nevertheless, the torque to weight ratio of FEFSMs reported to-date in the literature are still far below that required for EV application, unlike that of a PMFSM [71]. This characteristically low torque-to-weight ratio of FEFSM is overcome in the HEFSM, where both a secondary excitation coil and PM are used, albeit on a smaller volume. The main advantage of the HEFSM is a potentially much improved flux weakening capability, much higher power and torque densities, variable flux control capability, and higher operating efficiency [32],[44],[74]–[79].

2.6.1 HEFSM Topologies

To date, various combinations of stator slots and rotor poles for HEFSMs have been tried, some of them are illustrated in Figure 2.6. The 6S-4P HEFSM shown in Figure

2.6(a) is one of the earliest topologies that has been designed, where the PMs, DC FECs, and armature coils are arranged in three layers on the stator; with the armature coil placed in the innermost layer followed by DC FEC in the middle layer, and the PMs forming the outermost layer. A detailed explanation of the 6S-4P HEFSM is given in [80] and [81]. The 6S-4P HEFSM, unfortunately suffers from a low torque density and a high copper loss due to the long excitation coil ends. Wei Hua, M. Cheng and G. Zhang has managed to substantially reduce stator copper losses in the HEFSM by replacing the 6S-4P topology with a 12S-10P, where as shown in Figure 2.6(b) a FEC was used together with PMs of smaller dimensions [82].

In the alternative three-phase 12S-10P HEFSM topology proposed by E. Hoang et al. and shown in Figure 2.6(c) the FECs are located between the inner stator wall and the protruding bifurcated stator teeth [44],[83]. However, the machine suffered from a lower torque density due to the larger stator diameter required to accommodate the FECs. The original 12S-10P HEFSM design given in [44] has been improved and analyzed using finite element analysis. A significant high torque improvement has been achieved [32],[15]; unfortunately the efficiency of the machine is reduced due to the higher copper losses of the overlapping armature coil and FEC windings. On the other hand, the PMs in PMFSM topologies can be partially replaced by FEC windings and consequently, several HEFSM topologies were developed as in [84],[85]. Although they have no overlapped between the armature coil and FEC, the output torque capability is significantly reduced due to less PM volume.

Furthermore, from the 12S-10P E-core PMFSM mentioned in Figure 2.3(c) exhibits relatively higher torque density, a new HEFSM topology is proposed by inserting DC FECs at the middle teeth of the E-core stator shown in Figure 2.6(d) [86]. The outer diameter is kept similar as in 12S-10P E-core PMFSM and has delivered higher output torque density compared with the original E-core PMFSM.

All the HEFSMs mentioned above are having theta direction of armature coil and DC FEC that creates problem of PM flux cancellation at high FEC current density. More recently, a novel HEFSM with radial direction of FEC is developed as shown in Figure 2.6(e) to overcome the drawbacks of PM flux cancellation in the conventional series of PM and FEC slot in Figure 2.6(c) [78]. Obviously, the machine has performed good torque achievement and compete with the other HEFSMs.

With the abovementioned HEFSMs, the PMs on the stator may create the following problems:

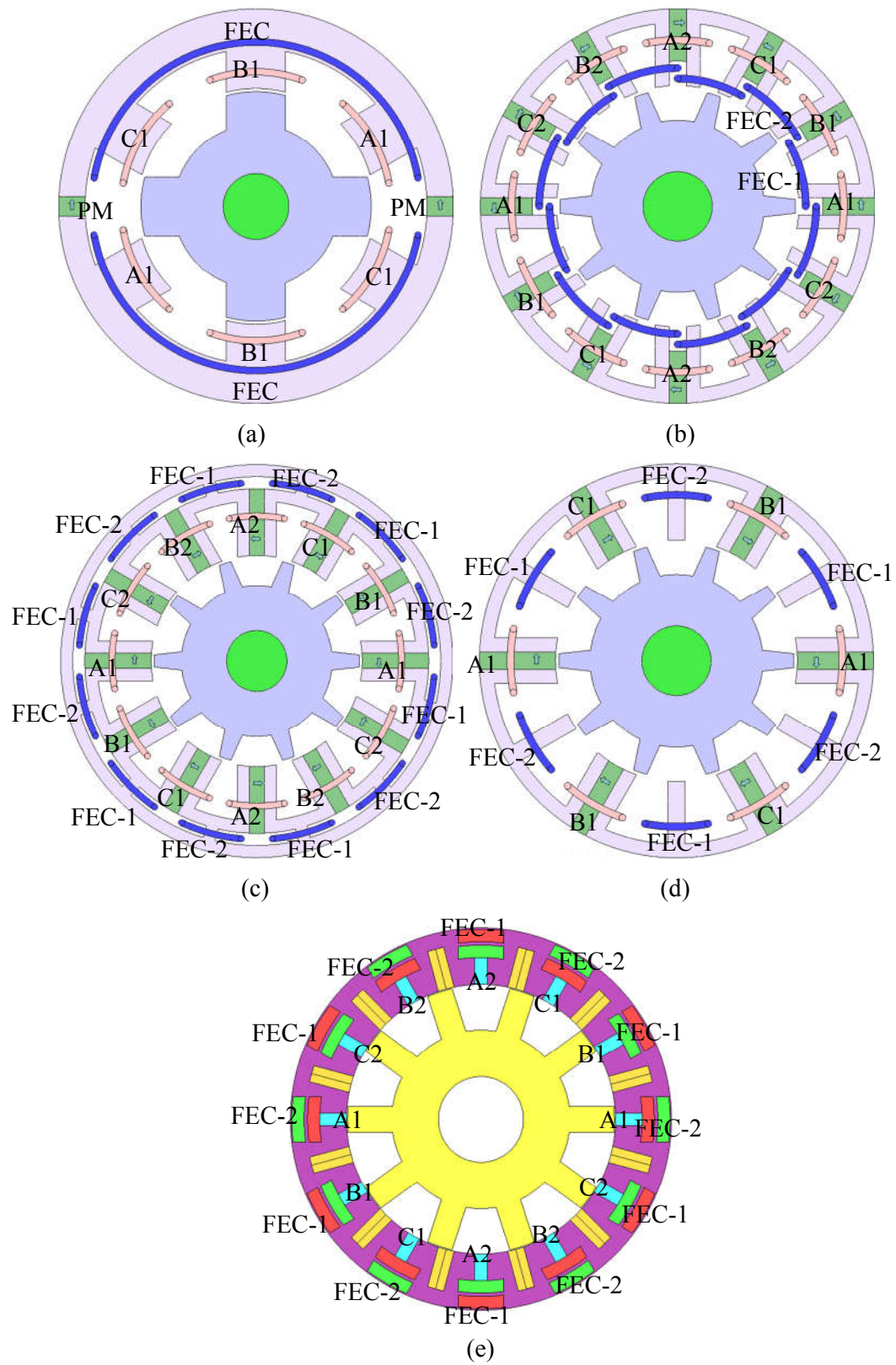


Figure 2.6: Example of HEFSMs (a) 6S-4P HEFSM (b) 12S-10P Inner FEC HEFSM (c) 12S-10P Outer FEC HEFSM (d) 12S-10P E-core HEFSM (e) Radial FEC HEFSM

- low permeability of the PM, Figure 2.6(a).
- (ii) The flux generated by PM is reduced by the flux path of DC FEC at high current density for high torque production, Figures 2.6(b) and (c).
 - (iii) Torque density may decrease due to less PM volume, Figure 2.6(d).
 - (iv) The stator segmented structure causes difficulty in the manufacturing process, Figures 2.6(b) and (d).
 - (v) Un-sinusoidal back-emf due to high harmonic content and insufficient stator yoke width between the armature coil slot and FEC slot resulting in flux saturation, thus reducing the optimal performance, Figure 2.6(e).
 - (vi) PMs are located along the stator radial of HEFSMs in Figures 2.6(a), (b), and (d), which has brought flux leakage outside and no contribution in torque production.

Based on various topologies discussed above, the 12S-10P HEFSM in Figure 2.6(c) with a single piece of stator and FEC at outermost stator body has brought advantages of high torque production, simple manufacturing process and is considered the best candidate to be further investigated. Therefore, the concept has been chosen and applied for the new topology of outer-rotor HEFSM proposed in this thesis.

2.6.2 Design of HEFSMs

The developed HEFSMs are mainly focused on providing variable speed-torque and constant power applications. In conventional PM machines, high torque and power densities are not the issue for a single operating point applications. In addition, there are much easier to manufacture and require no additional power converter for DC coils as in the HEFSMs. However, for variable speed applications, especially when used for EV or HEV, which requires wider speed range, the existence of hybrid excited flux sources are more essential in providing additional degree of freedom that can be used to enhance the efficiency in most operating regions. In this section, a design approach of hybrid excitation structures is briefly discussed. First, analytical modeling methods used in the design of hybrid excitation structures are presented. Then, the optimisation of HEFSM is discussed to clear up the applied methods.

Different analytical models, based on the formal solution of Maxwell equations have been developed in [87]–[90]. In [89], an analytical model has been used for a

series of hybrid excitation in which the formal solution of Maxwell equations are proposed. The main reason of this method is to reduce execution time and to enable the handling of variation parameters. While in the optimisation process, all the related parameters such as rotor pole depth, rotor pole width, PM depth, PM width, etc. are needed to be tested to deliver possible value for the best performance. However, it is considered that the iron permeability of the machines are infinity to solve the problem and magnetic saturation is not taken into consideration. If the magnetic saturation is to be considered, a model based on the equivalent magnetic circuit must be adopted. Some designs of the hybrid excitation machines that applied this technique have been discussed in [41],[91]–[94]. Nevertheless, due to the complex topology of the machines, it is quite difficult to set a proper equivalent model in which the right estimation must be made accordingly.

On the other hand, FEAs are broadly used to study and design not only for hybrid excitation machines but also for other types of machines. However, the main disadvantage of this approach is the time-consuming process to execute the design study especially for 3D design. Therefore, this technique normally takes longer to complete the design and optimisation process.

2.6.3 Outer-rotor flux switching machines

In recent years, research on in-wheel direct drive motor for EV propulsion system has become more attractive due to their several advantages. From forgoing literature obtained from [19],[95]–[97] stated that the in-wheel outer rotor machines have benefits of independent wheel controllability, higher torque density and efficiency over conventional inner-rotor structure. On the other side, the large space previously occupied by the necessary mechanical components such as transmission gear, speed reduction shafts, and differential in conventional EVs can be eliminated, thus reducing the overall weight of the vehicle and energy losses due to friction. However, most of the documented researches of outer-rotor machines are mainly discussed either in PMSMs or SRM [7],[19],[20]–[22],[96],[97]. However, due to the increasing cost of PM materials and problems of heat management in PMSMs, high torque ripple and acoustic noise problems of SRMs bring the opportunity for further investigation on outer-rotor machines to be applied for in-wheel direct drive EVs.

In the case of FSMs, the 12S-22P PMFSM is the earliest outer-rotor configuration that has been proposed only for light EV applications [23]. The design structure is illustrated in Figure 2.7. It has successfully attained sinusoidal back-emf and high torque at low speed. Nevertheless, constant PM flux of PMFSM makes it difficult to control, which requires field weakening flux control when operated beyond their base speed conditions. In addition, with the PM placed along the radial of the stator that might cause flux leakage and PM demagnetization effect, it should be avoided in field weakening operation [98]–[100]. Moreover, with the V-shaped stator, it is difficult to be optimized if the PM volume is kept constant. On the other hand, 36S-21P of WFFSM has been proposed as described in [38]. A segmented outer-rotor has been adopted to enhance the performance by effecting bi-directional flux flow. Thus, the machine is mechanically less robust, while huge size of machine is developed to attain high torque capability. Therefore, the machine is less suitable to be used for in-wheel direct drive EV applications.

Despite from numerous published documents and owing to the highlighted problems of outer-rotor FSMs, there appears to be an opportunity to investigate of outer-rotor HEFSM (OR-HEFSM) for in-wheel drive EV application. With the advantages of HEFSM as previously underlined, this thesis deals with a new structure of OR-HEFSM to overcome the above mentioned drawbacks.

Furthermore, because the optimal torque performance requires high current densities, good cooling system should be considered. An air-cooling system is not sufficient to keep the temperature of NdFeB within the allowable range (i.e. 150 °C) [69], because all the active parts of FSMs (namely the PMs and conductors) are located at the inner stator, and they operate with high current densities. Therefore, a more practical approach is to use a direct liquid cooling system previously proposed for outer-rotor machine, which effectively managed the temperature rise on the conductors and PMs [101]. High temperature superconducting windings with cooling containers [102] can also be considered.

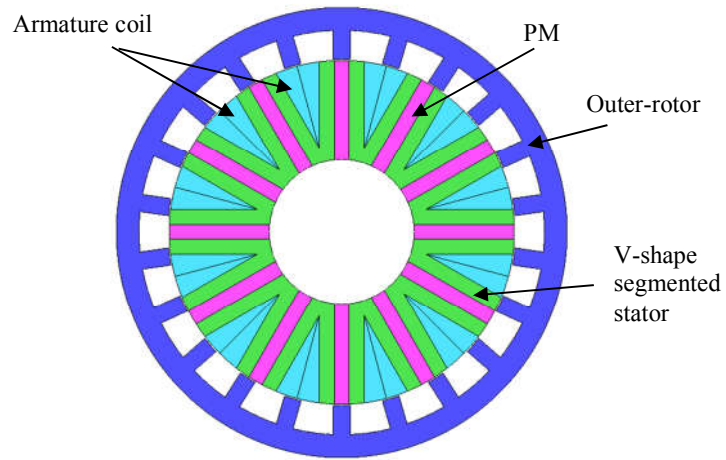


Figure 2.7: 12S-22P outer-rotor PMFSM [23].

2.6.4 Operating principle of OR-HEFSM

The term flux switching was introduced due to the excitation of the flux linkage, which switches the polarity as a result of the motion of the salient pole rotor. An in-depth operating principle of the proposed OR-HEFSM is illustrated in Figure 2.8, where the upper part is the salient rotor core while the lower part represents the stator body, which consists of PM, armature winding, and FEC winding. The excitation fluxes of both PM and FEC are indicated by the red and blue line, respectively. The polarity and the direction of both the PM and FEC fluxes are in the same manner, in which the rotor pole is receiving flux from the stator as shown in Figure 2.8(a). Both fluxes are combined and move together into the rotor, producing more fluxes called the hybrid excitation flux. When the rotor pole moves to the next stator teeth, as shown in Figure 2.8(b), the fluxes on the same rotor pole will leave for the current stator teeth, meaning that the polarity of the fluxes on the same rotor poles have changed. Furthermore, in Figures 2.8(c) and (d), the polarity of FEC is in a reverse direction, and only the flux of the PM flows into the rotor, whilst the flux of the FEC just moves around the FEC slot area, thus producing less flux excitation. The flux does not rotate but shifts

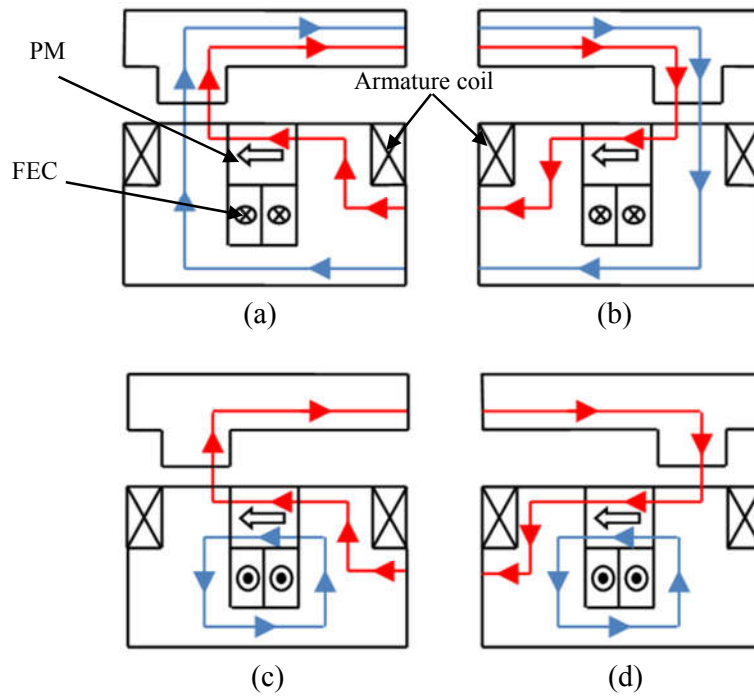


Figure 2.8: Principle operation of OR-HEFSM (a) $\theta_e = 0^\circ$ (b) $\theta_e = 180^\circ$ more excitation, (c) $\theta_e = 0^\circ$ (d) $\theta_e = 180^\circ$ less excitation.

clockwise and counter-clockwise in accordance with each armature current reversal. Therefore, the flux of PM can be easily controlled by DC FEC, in which it provides variable flux control capabilities even at field weakening and field strengthening conditions.

2.7 Dynamic model and equivalent circuit of OR-HEFSM

The OR-HEFSM can be modelled using general theory of PM synchronous machine to verify the original method of calculation. In PM synchronous motor, the PM is mounted on the rotor and armature winding is located in the stator while in FSM, both armature and PM are located in the stator, while for hybrid excitation there is an additional field excitation winding in the stator. The FSM completed two electrical cycles per revolution as opposed to the one by synchronous machine. The transformation of the state variables (voltages, current, and fluxes) from the uvw

stationary frame into the rotating dq0 coordinates, is accomplished by using the amplitude-invariant transformation matrix defined as in Equation (2.1) [93], [103].

$$\begin{bmatrix} x_d \\ x_q \\ x_0 \end{bmatrix} = \frac{2}{3} \begin{bmatrix} \cos(\theta) & \cos(\theta - \frac{2\pi}{3}) & \cos(\theta + \frac{2\pi}{3}) \\ -\sin(\theta) & -\sin(\theta - \frac{2\pi}{3}) & -\sin(\theta + \frac{2\pi}{3}) \\ \frac{1}{2} & \frac{1}{2} & \frac{1}{2} \end{bmatrix} \begin{bmatrix} x_u \\ x_v \\ x_w \end{bmatrix} \quad (2.1)$$

Where θ is the angle between the stator U- phase and field flux. On the contrary, the state variables in the uvw stationary frame can be obtained from the rotating dq0 components using the inverse amplitude-invariant transformation matrix;

$$\begin{bmatrix} x_u \\ x_v \\ x_w \end{bmatrix} = \begin{bmatrix} \cos(\theta) & -\sin(\theta) & 1 \\ \cos(\theta - \frac{2\pi}{3}) & -\sin(\theta - \frac{2\pi}{3}) & 1 \\ \cos(\theta + \frac{2\pi}{3}) & -\sin(\theta + \frac{2\pi}{3}) & 1 \end{bmatrix} \begin{bmatrix} x_d \\ x_q \\ x_0 \end{bmatrix} \quad (2.2)$$

For more accurate modelling, the implemented OR-HEFSM dynamic model takes into account the iron losses, specifically the eddy current losses. They are modelled by a resistor R_c , which is inserted in parallel with the magnetizing branch of the equivalent circuit, so that the power losses depended on the air-gap flux linkage [104]–[106]. Thus, the d-q axis currents of i_d and i_q are divided into iron loss currents (i_{cd} , i_{cq}) and magnetizing currents (i_{md} , i_{mq}), as shown in Figure 2.9, which is developed from the combination of PMSM and wound field synchronous machine (WFSM) [70],[103].

Assuming that the spatial distribution of flux density in air-gap under DC FEC and PM is sinusoidal and symmetrical three-phase sinusoidal current is fed to OR-HEFSM, d-q modelling approach for OR-HEFSM control similarly to conventional AC machines can be introduced. Taking into account the effects of magnetic saturation due to the increase in current and interference of each axis on each machine parameter,

REFERENCES

- [1] H. Ribberink and E. Entchev, "Electric vehicles - A 'one-size-fits-all' solution for emission reduction from transportation?," *2013 World Electr. Veh. Symp. Exhib. EVS 2014*, vol. 1, pp. 1–7, 2014.
- [2] S. Mehar, S. Zeadally, G. Remy, and S. M. Senouci, "Sustainable Transportation Management System for a Fleet of Electric Vehicles," *IEEE Trans. Intell. Transp. Syst.*, vol. 16, no. 3, pp. 1401–1414, 2015.
- [3] B. M. Al-Alawi and T. H. Bradley, "Review of hybrid, plug-in hybrid, and electric vehicle market modeling Studies," *Renewable and Sustainable Energy Reviews*, vol. 21, pp. 190–203, 2013.
- [4] D. B. Richardson, "Electric vehicles and the electric grid: A review of modeling approaches, Impacts, and renewable energy integration," *Renewable and Sustainable Energy Reviews*, vol. 19, pp. 247–254, 2013.
- [5] M. A. Hannan, F. A. Azidin, and A. Mohamed, "Hybrid electric vehicles and their challenges: A review," *Renewable and Sustainable Energy Reviews*, vol. 29, pp. 135–150, 2014.
- [6] K. Rahman, N. Patel, T. Ward, J. Nagashima, F. Caricchi, and F. Crescimbin, "Application of direct drive wheel motor for fuel cell electric and hybrid electric vehicle propulsion system," *IEEE Trans. Ind. Appl.*, vol. 42, no. 5, pp. 1185–1192, 2006.
- [7] C. J. Ifedi, B. C. Mecrow, S. T. M. Brockway, G. S. Boast, G. J. Atkinson, and D. Kostic-Perovic, "Fault-tolerant in-wheel motor topologies for high-performance electric vehicles," *IEEE Trans. Ind. Appl.*, vol. 49, pp. 1249–1257, 2013.
- [8] T. Sutikno, N. R. N. Idris, and A. Jidin, "A review of direct torque control of induction motors for sustainable reliability and energy efficient drives," *Renewable and Sustainable Energy Reviews*, vol. 32, pp. 548–558, 2014.

- [9] C. C. Chan, "The state of the art of electric, hybrid, and fuel cell vehicles," *Proc. IEEE*, vol. 95, pp. 704–718, 2007.
- [10] Z. Q. Zhu and D. Howe, "Electrical Machines and Drives for Electric, Hybrid, and Fuel Cell Vehicles," *Proc. IEEE*, vol. 95, no. 4, 2007.
- [11] Z. Q. Zhu, Y. J. Zhou, and J. T. Chen, "Electromagnetic Performance of Nonoverlapping Stator Wound Field Synchronous Machine with Salient Pole Rotor," *IEEE Trans. Magn.*, vol. 51, no. 11, pp. 10–13, 2015.
- [12] C. Sanabria-Walter, H. Polinder, and J. A. Ferreira, "High-Torque-Density High-Efficiency Flux-Switching PM Machine for Aerospace Applications," *Emerg. Sel. Top. Power Electron. IEEE J.*, vol. 1, no. 4, pp. 327–336, 2013.
- [13] J. R. Riba, C. López-Torres, L. Romeral, and A. Garcia, "Rare-earth-free propulsion motors for electric vehicles: A technology review," *Renewable and Sustainable Energy Reviews*, vol. 57, pp. 367–379, 2016.
- [14] I. Ozawa, T. Kosaka, and N. Matsui, "Less rare-earth magnet-high power density hybrid excitation motor designed for Hybrid Electric Vehicle drives," *Power Electron. Appl. 2009. EPE '09. 13th Eur. Conf.*, no. 1, pp. 1–10, 2009.
- [15] E. Sulaiman, T. Kosaka, and N. Matsui, "Design Optimisation of 12Slot – 10Pole Hybrid Excitation Flux Switching Synchronous Machine with 0.4kg Permanent Magnet for Hybrid Electric Vehicles," in *8th International Conference on Power Electronics*, pp. 1913–1920, 2011,
- [16] Y. Li, W. Xu, and S. Member, "Optimisation and Performance Analysis of E-Core Machines for Electric Vehicle Applications," in *17th International Conference on Electrical Machines and Systems (ICEMS)*, pp. 53–59, 2014.
- [17] S. Hlioui, Y. Amara, E. Hoang, and M. Gabsi, "Overview of hybrid excitation synchronous machines technology," in *2013 International Conference on Electrical Engineering and Software Applications, ICEESA 2013*, pp. 1–10, 2013.
- [18] Y. Amara, L. Vido, M. Gabsi, E. Hoang, M. Lecrivain, and F. Chabot, "Hybrid Excitation Synchronous Machines: Energy Efficient Solution for Vehicle Propulsion," *2006 IEEE Veh. Power Propuls. Conf.*, vol. 58, no. 5, pp. 1–6, 2006.
- [19] A. Labak and N. C. Kar, "Outer rotor switched reluctance motor design for in-wheel drive of electric bus applications," *Proc. - 2012 20th Int. Conf. Electr.*

- Mach. ICEM 2012*, pp. 418–423, 2012.
- [20] K. T. Chau, D. Zhang, J. Z. Jiang, C. Liu, and Y. Zhang, “Design of a magnetic-geared outer-rotor permanent-magnet brushless motor for electric vehicles,” *IEEE Trans. Magn.*, vol. 43, no. 6, pp. 2504–2506, 2007.
- [21] S. Yang, N. J. Baker, B. C. Mecrow, C. Hilton, G. Sooriyakumar, D. Kostic-Perovic, and A. Fraser, “Cost reduction of a permanent magnet in-wheel electric vehicle traction motor,” *Proc. - 2014 Int. Conf. Electr. Mach. ICEM 2014*, pp. 443–449, 2014.
- [22] M. Morishita, I. Miki, and M. Nakamura, “Efficiency improvement for IPMSM of outer rotor type,” in *SPEEDAM 2010 - International Symposium on Power Electronics, Electrical Drives, Automation and Motion*, pp. 115–118, 2010.
- [23] W. Fei, P. C. K. Luk, J. X. Shen, Y. Wang, and M. Jin, “A novel permanent-magnet flux switching machine with an outer-rotor configuration for in-wheel light traction applications,” *IEEE Trans. Ind. Appl.*, vol. 48, no. 5, pp. 1496–1506, 2012.
- [24] W. Y. Huang, A. Bettayeb, R. Kaczmarek, and J. C. Vannier, “Optimization of magnet segmentation for reduction of eddy-current losses in permanent magnet synchronous machine,” *IEEE Trans. Energy Convers.*, vol. 25, no. 2, pp. 381–387, 2010.
- [25] M. Kamiya, “Development of Traction Drive Motors for the Toyota Hybrid System,” *IEEJ Trans. Ind. Appl.*, vol. 126, no. 4, pp. 473–479, 2006.
- [26] V. I. Patel and J. Wang, “Assessment of 12-slot, 14-pole permanent magnet flux switching machine with hybrid excitation for electric vehicle application,” in *2013 IEEE Energy Conversion Congress and Exposition, ECCE 2013*, pp. 5092–5099, 2013.
- [27] I. A. Somesan, L.E. and Viorel, “Keywords PMFSM Structure and Dedicated Algorithm,” *Power Eng. Electr. Eng.*, vol. 11, no. 2, pp. 46–53, 2013.
- [28] W.-Z. Fei, J.-X. Shen, C.-F. Wang, and P. C.-K. Luk, “Design and analysis of a new outer-rotor permanent-magnet flux-switching machine for electric vehicle propulsion,” *Int. J. Comput. Math. Electr. Electron. Eng.*, vol. 30, no. 1, pp. 48–61, 2011.
- [29] A. E. Laws, “An electromechanical transducer with permanent magnet polarization,” *Tech. Note No. G.W.202, R. Aircr. Establ. Farnborough, UK*,

1952, 1952.

- [30] S. E. Rauch and L. J. Johnson, "Design Principles of Flux-Switch Alternators," *Trans. Am. Inst. Electr. Eng. Part III Power Appar. Syst.*, vol. 74, no. December, pp. 1261–1268, 1955.
- [31] E. Hoang, A. H. Ben-Ahmed, and J. Lucidarme, "Switching Flux Permanent Magnet Poly-Phased Synchronous Machines," in *Proceeding of 7th European Conference on Power Electronics and Applications (EPE)*, vol. 3, pp. 903–908, 1997.
- [32] E. Sulaiman, T. Kosaka, and N. Matsui, "Design and analysis of high-power/high-torque density dual excitation switched-flux machine for traction drive in HEVs," *Renew. Sustain. Energy Rev.*, vol. 34, pp. 517–524, 2014.
- [33] Z. Q. Zhu and D. Evans, "Overview of recent advances in innovative electrical machines - With particular reference to magnetically geared switched flux machines," in *2014 17th International Conference on Electrical Machines and Systems, ICEMS 2014*, 2015.
- [34] F. Khan, and E. Sulaiman, "Design Optimization and Efficiency Analysis of 12Slot-10Pole Wound Field Flux Switching Machine.," in *IEEE Magnetics Conference (INTERMAG)*, pp. 1–1, 2015.
- [35] M. Lin, L. Hao, X. Li, X. Zhao, and Z. Q. Zhu, "A novel axial field flux-switching permanent magnet wind power generator," *IEEE Trans. Magn.*, vol. 47, no. 10, pp. 4457–4460, 2011.
- [36] W. X. W. Xu, J. Z. J. Zhu, Y. Z. Y. Zhang, Y. W. Y. Wang, Y. L. Y. Li, and J. H. J. Hu, "Flux-switching permanent magnet machine drive system for plug-in hybrid electrical vehicle," *Univ. Power Eng. Conf. (AUPEC), 2010 20th Australas.*, 2010.
- [37] W. Hua, X. Yin, G. Zhang, and M. Cheng, "Analysis of two novel five-phase hybrid-excitation flux-switching machines for electric vehicles," *IEEE Trans. Magn.*, vol. 50, no. 11, 2014.
- [38] M. Galea, C. Gerada, and T. Hamiti, "Design considerations for an outer rotor, field wound, flux switching machine," *Proc. - 2012 20th Int. Conf. Electr. Mach. ICEM 2012*, pp. 171–176, 2012.
- [39] Y. Tang, J. J. H. Paulides, T. E. Motosca, and E. a. Lomonova, "Flux-switching machine with DC excitation," *IEEE Trans. Magn.*, vol. 48, no. 11, pp. 3583–

- 3586, 2012.
- [40] K. T. Chau and C. C. Chan, “Static characteristics of a new doubly salient permanent magnet motor,” *IEEE Trans. Energy Convers.*, vol. 16, no. 1, pp. 20–25, 2001.
- [41] E. Hoang, M. Gabsi, M. Lecrivain, and B. Multon, “Influence of magnetic losses on maximum power limits of synchronous permanent magnet drives in flux-weakening mode,” *Industry Applications Conference, 2000. Conference Record of the 2000 IEEE*, vol. 1, pp. 299–303 vol.1, 2000.
- [42] Z. Q. Zhu and J. T. Chen, “Advanced flux-switching permanent magnet brushless machines,” *IEEE Trans. Magn.*, vol. 46, no. 6, pp. 1447–1453, 2010.
- [43] F. Li, W. Hua, M. Tong, G. Zhao, and M. Cheng, “Nine-Phase Flux-Switching Permanent Magnet Brushless,” *IEEE Trans. Magn.*, vol. 51, no. 3, pp. 34–37, 2015.
- [44] M. G. E. Hoang, M. Lecrivain, “A New Structure of a Switching Flux Synchronous Polyphased Machine,” in *European Conference on Power Electronics and Applications*, no. 33, pp. 1–8, 2007.
- [45] J. Wang, W. Wang, K. Atallah, and D. Howe, “Design considerations for tubular flux-switching permanent magnet machines,” in *IEEE Transactions on Magnetics*, vol. 44, no. 11 PART 2, pp. 4026–4032, 2008.
- [46] C. F. Wang, J. X. Shen, Y. Wang, L. L. Wang, and M. J. Jin, “A new method for reduction of detent force in permanent magnet flux-switching linear motors,” *IEEE Trans. Magn.*, vol. 45, no. 6, pp. 2843–2846, 2009.
- [47] S. Xu, W. Zhao, J. Ji, Y. Du, D. Zhang, and G. Liu, “Thrust ripple reduction of linear flux-switching PM motor using harmonic injected current,” *2013 Int. Conf. Electr. Mach. Syst. ICEMS 2013*, pp. 1886–1889, 2013.
- [48] and M. C. X. Xue, W. Zhao, J. Zhu, G. Liu, X. Zhu, “Design of five-phase modular flux-switching permanent-magnet machines for high reliability applications,” *IEEE Trans. Intell. Transp. Syst.*, vol. 49, no. 7, pp. 3491–3944, 2013.
- [49] L. Papini, T. Raminosa, D. Gerada, and C. Gerada, “A high-speed permanent-magnet machine for fault-tolerant drivetrains,” *IEEE Trans. Ind. Electron.*, vol. 61, pp. 3071–3080, 2014.
- [50] H. Liu, W. Zhao, J. Ji, Y. Du, H. Zhou, and D. Zhang, “Fault-tolerant control

- of modular linear flux-switching permanent-magnet motor,” *2013 Int. Conf. Electr. Mach. Syst. ICEMS 2013*, pp. 1890–1894, 2013.
- [51] L. Hao, M. Lin, X. Zhao, X. Fu, Z. Q. Zhu, and P. Jin, “Static characteristics analysis and experimental study of a novel axial field flux-switching permanent magnet generator,” *IEEE Trans. Magn.*, vol. 48, no. 11, pp. 4212–4215, 2012.
- [52] L. Hao, M. Lin, X. Zhao, and H. Luo, “Analysis and optimization of EMF waveform of a novel axial field flux-switching permanent magnet machine,” *2011 Int. Conf. Electr. Mach. Syst. ICEMS 2011*, pp. 1–6, 2011.
- [53] R. L. Owen, Z. Q. Zhu, A. S. Thomas, G. W. Jewell, and D. Howe, “Fault-tolerant flux-switching permanent magnet brushless AC machines,” in *Conference Record - IAS Annual Meeting (IEEE Industry Applications Society)*, 2008.
- [54] W. Zhang, M. Y. Lin, L. Hao, L. C. Tai, and Z. G. Pei, “Design and Analysis of a Novel E-Core Axial Field Flux-Switching Permanent Magnet Machine,” *Appl. Mech. Mater.*, vol. 416–417, pp. 175–180, 2013.
- [55] F. Xiao, X. Liu, Y. Du, K. Shi, and P. Xu, “A C-core linear flux-switching permanent magnet machine with positive additional teeth,” *2014 17th Int. Conf. Electr. Mach. Syst. ICEMS 2014*, pp. 1757–1761, 2015.
- [56] and M. A. A. Zulu, B. C. Mecrow, “Investigation of the dq equivalent model for performance prediction FSM PM with segmental rotor.pdf.crdownload,” *IEEE Trans. Magn.*, vol. 59, no. 6, pp. 2393–2402, 2012.
- [57] J. T. Chen, Z. Q. Zhu, and D. Howe, “Stator and rotor pole combinations for multi-tooth flux-switching permanent-magnet brushless AC machines,” *IEEE Trans. Magn.*, vol. 44, no. 12, pp. 4659–4667, 2008.
- [58] Z. Q. Zhu, J. T. Chen, Y. Pang, D. Howe, S. Iwasaki, and R. Deodhar, “Analysis of a novel multi-tooth flux-switching PM brushless AC machine for high torque direct-drive applications,” in *IEEE Transactions on Magnetism*, vol. 44, no. 11 PART 2, pp. 4313–4316, 2008.
- [59] J. Cai, Q. Lu, Y. Jin, C. Chen, and Y. Ye, “Performance Investigation of Multi-Tooth Flux-switching PM Linear Motor,” in *International Conference on Electrical Machines and Systems (ICEMS), 2011*, pp. 1 – 6, 2011.
- [60] Z. Q. Zhu, Y. Pang, D. Howe, S. Iwasaki, R. Deodhar, and A. Pride, “Analysis of electromagnetic performance of flux-switching permanent-magnet machines

- by nonlinear adaptive lumped parameter magnetic circuit model,” *IEEE Trans. Magn.*, vol. 41, no. 11, pp. 4277–4287, 2005.
- [61] J. Yang, Q. Ma, Y. Deng, and Y. Liu, “Flux-weakening capability of flux-switching permanent magnet motor,” in *2010 International Conference on E-Product E-Service and E-Entertainment, ICEEE2010*, 2010.
- [62] J. T. Chen, Z. Q. Zhu, S. Iwasaki, and R. P. Deodhar, “A novel E-core switched-flux PM brushless AC machine,” *IEEE Trans. Ind. Appl.*, vol. 47, no. 3, pp. 1273–1282, 2011.
- [63] J. T. Chen, Z. Q. Zhu, S. Iwasaki, and R. P. Deodhar, “Comparison of losses and efficiency in alternate flux-switching permanent magnet machines,” in *19th International Conference on Electrical Machines, ICEM 2010*, 2010.
- [64] J. H. Walker, “The theory of the inductor alternator,” *J. Inst. Electr. Eng. - Part II Power Eng.*, vol. 89, no. 9, pp. 227–241, 1942.
- [65] D. A. Torrey, “Switched reluctance generators and their control,” *IEEE Trans. Ind. Electron.*, vol. 49, no. 1, pp. 3–14, 2002.
- [66] Y. J. Zhou, Z. Q. Zhu, and S. Sheffield, “Comparison of Low-Cost Wound-Field Switched-Flux Machines,” *IEEE Trans. Ind. Appl.*, vol. 50, no. 5, pp. 904–911, 2013.
- [67] C. Pollock and M. Wallace, “The flux switching motor, a DC motor without magnets or brushes,” *Conf. Rec. 1999 IEEE Ind. Appl. Conf. Thirty-Forth IAS Annu. Meet. (Cat. No.99CH36370)*, vol. 3, pp. 1980–1987, 1999.
- [68] C. Pollock, H. Pollock, R. Barron, J. R. Coles, D. Moule, A. Court, and R. Sutton, “Flux-switching motors for automotive applications,” *IEEE Trans. Ind. Appl.*, vol. 42, no. 5, pp. 1177–1184, 2006.
- [69] J. T. Chen, Z. Q. Zhu, S. Iwasaki, and R. Deodhar, “Low cost flux-switching brushless AC machines,” in *2010 IEEE Vehicle Power and Propulsion Conference, VPPC 2010*, 2010.
- [70] A. Zulu, B. C. Mecrow, and M. Armstrong, “A wound-field three-phase flux-switching synchronous motor with all excitation sources on the stator,” *IEEE Trans. Ind. Appl.*, vol. 46, no. 6, pp. 2363–2371, 2010.
- [71] E. Sulaiman, T. Kosaka, and N. Matsui, “Design study and experimental analysis of wound field flux switching motor for HEV applications,” in *Proceedings - 2012 20th International Conference on Electrical Machines*,

- ICEM 2012*, pp. 1269–1275, 2012.
- [72] F. Khan, E. Sulaiman, M. Z. Ahmad, and Z. A. Husin, “Design and Analysis of Wound Field Three-Phase Flux Switching Machine with Non-overlap Windings and Salient Rotor,” *Int. J. Electr. Eng. Informatics*, vol. 7, no. 2, pp. 323–333, 2015.
- [73] F. Khan, M. Z. Ahmad, and E. Sulaiman, “A novel wound field flux switching machine with salient pole rotor and non- overlapping windings,” *Turkish J. Electr. Eng. Comput. Sci.*, no. 199, pp. 1–25, 2016.
- [74] Y. Amara, L. Vido, M. Gabsi, E. Hoang, H. A. Ben Ahmed, and M. Lecrivain, “Hybrid excitation synchronous machines: Energy-efficient solution for vehicles propulsion,” *IEEE Trans. Veh. Technol.*, vol. 58, no. 5, pp. 2137–2149, 2009.
- [75] C. Z. C. Zhao and Y. Y. Y. Yan, “A review of development of hybrid excitation synchronous machine,” *Proc. IEEE Int. Symp. Ind. Electron. 2005. ISIE 2005.*, vol. 2, pp. 857–862, 2005.
- [76] Z. Sun, J. Wang, G. W. Jewell, and D. Howe, “Enhanced optimal torque control of fault-tolerant PM machine under flux-weakening operation,” *IEEE Trans. Ind. Electron.*, vol. 57, no. 1, pp. 344–353, 2010.
- [77] S. N. U. Zakaria and E. Sulaiman, “Magnetic flux analysis of E-core hybrid excitation flux switching motor with various topologies,” in *IEEE Asia-Pacific Conference on Applied Electromagnetics (APACE)*, pp. 95–98, 2014.
- [78] S. K. Rahimi and E. Sulaiman, “Design investigation of hybrid excitation flux switching machine for high-speed electric vehicles,” in *Proceedings of the 2014 IEEE 8th International Power Engineering and Optimization Conference, PEOCO 2014*, no. March, pp. 303–307, 2014.
- [79] H. Nakane, T. Kosaka, and N. Matsui, “Design Studies on Hybrid Excitation of Flux Switching Motor with High Power and Torque Densities for HEV Applications,” in *IEEE International Electric Machines & Drive Conference*, pp. 234–239, 2015.
- [80] Y. Liao, F. Liang, and T. A. Lipo, “Novel permanent magnet motor with doubly salient structure,” *IEEE Trans. Ind. Appl.*, vol. 31, no. 5, pp. 1069–1078, 1995.
- [81] K. T. Chau, M. Cheng, and C. C. Chan, “Nonlinear magnetic circuit analysis for a novel stator doubly fed doubly salient machine,” in *IEEE Transactions on*

- Magnetics*, vol. 38, no. 5 I, pp. 2382–2384, 2002.
- [82] W. Hua, M. Cheng, and G. Zhang, “A novel hybrid excitation flux-switching motor for hybrid vehicles,” in *IEEE Transactions on Magnetics*, vol. 45, no. 10, pp. 4728–4731, 2009.
- [83] E. Hoang, S. Hlioui, M. Lecrivain, and M. Gabsi, “Experimental comparison of lamination material (M330-50 & NO20) case switching flux synchronous machine with hybrid excitation,” *EPE J. (European Power Electron. Drives Journal)*, vol. 20, no. 3, pp. 28–33, 2010.
- [84] R. L. Owen, Z. Q. Zhu, and G. W. Jewell, “Hybrid-excited flux-switching permanent-magnet machines with iron flux bridges,” in *IEEE Transactions on Magnetics*, vol. 46, no. 6, pp. 1726–1729, 2010.
- [85] N. A. Jafar and E. Sulaiman, “Design analysis of 12S-10P hybrid-excitation flux-switching permanent-magnet machines for hybrid electric vehicle,” *Proc. 2014 IEEE 8th Int. Power Eng. Optim. Conf. PEOCO 2014*, no. March, pp. 308–312, 2014.
- [86] J. T. Chen, Z. Q. Zhu, S. Iwasaki, and R. P. Deodhar, “A novel hybrid-excited switched-flux brushless AC machine for EV/HEV applications,” *IEEE Trans. Veh. Technol.*, vol. 60, no. 4, pp. 1365–1373, 2011.
- [87] Y. Amara, S. Hlioui, R. Belfkira, G. Barakat, and M. Gabsi, “Comparison of open circuit flux control capability of a series double excitation machine and a parallel double excitation machine,” *IEEE Trans. Veh. Technol.*, vol. 60, no. 9, pp. 4194–4207, 2011.
- [88] H. Bali, Y. Amara, G. Barakat, R. Ibtouen, and M. Gabsi, “Analytical modeling of open circuit magnetic field in wound field and series double excitation synchronous machines,” *IEEE Trans. Magn.*, vol. 46, no. 10, pp. 3802–3815, 2010.
- [89] A. Bellara, H. Bali, R. Belfkira, Y. Amara, and G. Barakat, “Analytical prediction of open-circuit eddy-current loss in series double excitation synchronous machines,” *IEEE Trans. Magn.*, vol. 47, no. 9, pp. 2261–2268, 2011.
- [90] B. Kamel, I. Rachid, and L. Thierry, “Analytical prediction of magnetic field in parallel double excitation and spoke-type permanent-magnet machines accounting for tooth-tips and shape of polar pieces,” *IEEE Trans. Magn.*, vol.

- 48, no. 7, pp. 2121–2137, 2012.
- [91] D. Fodorean, A. Djerdir, I. A. Viorel, and A. Miraoui, “A double excited synchronous machine for direct drive application-design and prototype tests,” *IEEE Trans. Energy Convers.*, vol. 22, no. 3, pp. 656–665, 2007.
- [92] X. Liu, H. Lin, Z. Q. Zhu, C. Yang, S. Fang, and J. Guo, “A novel dual-stator hybrid excited synchronous wind generator,” *IEEE Trans. Ind. Appl.*, vol. 45, no. 3, pp. 947–953, 2009.
- [93] S. Hlioui, L. Vido, Y. Amara, M. Gabsi, a. Miraoui, and M. Lécrivain, “Magnetic equivalent circuit model of a hybrid excitation synchronous machine,” *COMPEL Int. J. Comput. Math. Electr. Electron. Eng.*, vol. 27, no. 5, pp. 1000–1015, 2008.
- [94] B. Nedjar, S. Hlioui, L. Vido, Y. Amara, and M. Gabsi, “Hybrid Excitation Synchronous Machine modeling using magnetic equivalent circuits,” *2011 International Conference on Electrical Machines and Systems*. pp. 1–6, 2011.
- [95] X. D. Xue, K. W. E. Cheng, S. Member, T. W. Ng, and N. C. Cheung, “Multi-Objective Optimization Design of In-Wheel Switched Reluctance Motors in Electric Vehicles,” *Ieee Trans. Ind. Electron. Vol. 57, No. 9, Sept. 2010*, vol. 57, no. 9, pp. 2980–2987, 2010.
- [96] C. Liu, “Design of a new outer-rotor flux-controllable vernier PM in-wheel motor drive for electric vehicle,” in *2011 International Conference on Electrical Machines and Systems, ICEMS 2011*, 2011.
- [97] J. L. J. Lin, K. W. E. Cheng, Z. Z. Z. Zhang, and X. X. X. Xue, “Experimental investigation of in-wheel switched reluctance motor driving system for future electric vehicles,” *2009 3rd Int. Conf. Power Electron. Syst. Appl.*, pp. 3–8, 2009.
- [98] J. D. McFarland, T. M. Jahns, and A. M. El-Refaeie, “Demagnetization performance characteristics of flux switching permanent magnet machines,” in *Proceedings - 2014 International Conference on Electrical Machines, ICEM 2014*, 2014, pp. 2001–2007.
- [99] B. Ebrahimi and J. Faiz, “Demagnetization Fault Diagnosis in Surface Mounted Permanent Magnet Synchronous Motors,” *IEEE Trans. Magn.*, vol. 49, no. 3, pp. 1–1, 2012.
- [100] J. Hong, S. Park, D. Hyun, T. J. Kang, S. Bin Lee, C. Kral, and A. Haumer,

- “Detection and classification of rotor demagnetization and eccentricity faults for PM synchronous motors,” *IEEE Trans. Ind. Appl.*, vol. 48, no. 3, pp. 923–932, 2012.
- [101] M. Polikarpova, P. Ponomarev, P. R oytt a, S. Semken, Y. Alexandrova, and J. Pyrh onen, “Direct liquid cooling for an outer-rotor direct-drive permanent-magnet synchronous generator for wind farm applications,” *IET Electr. Power Appl.*, vol. 9, no. 8, pp. 523–532, 2015.
- [102] F. Machines, J. Rao, W. Xu, and S. Member, “Modular Stator High Temperature Superconducting,” *IEEE Trans. Appl. Supercond.*, vol. 24, no. 5, pp. 1–5, 2014.
- [103] J. Jung, J. Lee, S. Kwon, J. Hong, and K. Kim, “Equivalent circuit analysis of interior permanent magnet synchronous motor considering magnetic saturation,” *Electr. Veh. Symp.*, vol. 3, pp. 1–5, 2009.
- [104] J. A. G emes, A. M. Iraolagoitia, J. I. Del Hoyo, and P. Fern andez, “Torque analysis in permanent-magnet synchronous motors: A comparative study,” *IEEE Trans. Energy Convers.*, vol. 26, no. 1, pp. 55–63, 2011.
- [105] M.-F. Hsieh and Y.-C. Hsu, “A Generalized Magnetic Circuit Modeling Approach for Design of Surface Permanent-Magnet Machines,” *IEEE Trans. Ind. Electron.*, vol. 59, no. 2, pp. 779–792, 2012.
- [106] G. Heins, M. Thiele, and T. Brown, “Accurate torque ripple measurement for PMSM,” *IEEE Trans. Instrum. Meas.*, vol. 60, no. 12, pp. 3868–3874, 2011.
- [107] Y. H. Yeh, M. F. Hsieh, and D. G. Dorrell, “Different arrangements for dual-rotor dual-output radial-flux motors,” in *IEEE Transactions on Industry Applications*, vol. 48, no. 2, pp. 612–622, 2012.
- [108] D. Wang, X. Wang, D. Qiao, Y. Pei, and S. Y. Jung, “Reducing cogging torque in surface-mounted permanent-magnet motors by nonuniformly distributed teeth method,” *IEEE Trans. Magn.*, vol. 47, no. 9, pp. 2231–2239, 2011.
- [109] L. Hao, M. Lin, D. Xu, N. Li, and W. Zhang, “Cogging Torque Reduction of Axial-Field Flux-Switching Permanent Magnet Machine by Rotor Tooth Notching,” *IEEE Trans. Magn.*, vol. 51, no. 11, 2015.
- [110] L. Hao, M. Lin, D. Xu, and W. Zhang, “Cogging torque reduction of axial field flux-switching permanent magnet machine by adding magnetic bridge in stator tooth,” *IEEE Trans. Appl. Supercond.*, vol. 24, no. 3, pp. 1–5, 2014.

- [111] W. Fei, P. C. K. Luk, and J. Shen, "Torque analysis of permanent-magnet flux switching machines with rotor step skewing," *IEEE Trans. Magn.*, vol. 48, no. 10, pp. 2664–2673, 2012.
- [112] W. Fei, P. C. K. Luk, J. X. Shen, B. Xia, and Y. Wang, "Permanent-magnet flux-switching integrated starter generator with different rotor configurations for cogging torque and torque ripple mitigations," *IEEE Trans. Ind. Appl.*, vol. 47, no. 3, pp. 1247–1256, 2011.
- [113] D. Wang, X. Wang, and S. Y. Jung, "Reduction on cogging torque in flux-switching permanent magnet machine by teeth notching schemes," *IEEE Trans. Magn.*, vol. 48, no. 11, pp. 4228–4231, 2012.
- [114] S. E. Abdollahi and S. Vaez-Zadeh, "Reducing cogging torque in flux switching motors with segmented rotor," *IEEE Trans. Magn.*, vol. 49, no. 10, pp. 5304–5309, 2013.
- [115] D. N. Dyck and D. A. Lowther, "Automated design of magnetic devices by optimizing material distribution," *IEEE Trans. Magn.*, vol. 32, no. 3 PART 2, pp. 1188–1192, 1996.
- [116] J. Byun and S. Hahn, "Topology Optimization of Electrical Devices Using Mutual Energy and Sensitivity," *IEEE Trans. Magn.*, vol. 35, no. 5, pp. 3718–3720, 1999.
- [117] Chang-Hwan Im, Hyun-Kyo Jung, and Yong-Joo Kim, "Hybrid genetic algorithm for electromagnetic topology optimization," *IEEE Trans. Magn.*, vol. 39, no. 5, pp. 2163–2169, 2003.
- [118] S. Wang, D. Youn, H. Moon, and J. Kang, "Topology optimization of electromagnetic systems considering magnetization direction," *IEEE Trans. Magn.*, vol. 41, no. 5, pp. 1808–1811, 2005.
- [119] D. Iles-klumpner, M. Risticvic, and I. Boldea, "Advanced Optimization Design Techniques for Automotive Interior Permanent Magnet Synchronous Machines," in *IEEE International Conference on Electric Machines and Drives*, pp. 227–234, 2005,.
- [120] D. H. Kim, J. K. Sykulski, and D. A. Lowther, "The implications of the use of composite materials in electromagnetic device topology and shape optimization," *IEEE Trans. Magn.*, vol. 45, no. 3, pp. 1154–1157, 2009.
- [121] J. S. Choi and J. Yoo, "Structural Topology Optimization of Magnetic Actuators

- Using Genetic Algorithms and ON / OFF Sensitivity,” vol. 45, no. 5, pp. 2276–2279, 2009.
- [122] N. Takahashi, T. Yamada, and D. Miyagi, “Examination of optimal design of IPM motor using ON/OFF method,” *IEEE Trans. Magn.*, vol. 46, no. 8, pp. 3149–3152, 2010.
- [123] M. Risticevic, D. Iles, A. Moeckel, and R. B. Gmbh, “Design of an Interior Permanent Magnet Synchronous Motor supported by the Topology Optimization Algorithm,” in *International Symposium on Power Electronics, Electrical Drives, Automation and Motion*, pp. 221–225, 2016.
- [124] E. Sulaiman, T. Kosaka, and N. Matsui, “High power density design of 6-slot-8-pole hybrid excitation flux switching machine for hybrid electric vehicles,” in *IEEE Transactions on Magnetics*, vol. 47, pp. 4453–4456, 2011.
- [125] M. Kamachi, H. Miyamoto, and Y. Sano, “Development of power management system for electric vehicle ‘i-MiEV,’” *2010 Int. Power Electron. Conf. - ECCE ASIA -*, pp. 2949–2955, 2010.
- [126] D. Gerada, A. Mebarki, N. L. Brown, and C. Gerada, “Optimal split ratio for high speed induction machines,” in *2010 IEEE Energy Conversion Congress and Exposition, ECCE 2010 - Proceedings*, pp. 10–16, 2010.
- [127] Y. Shen and Z. Q. Zhu, “Analytical prediction of optimal split ratio for fractional-slot external rotor PM brushless machines,” in *IEEE Transactions on Magnetics*, vol. 47, no. 10, pp. 4187–4190, 2011.
- [128] E. Sulaiman, “Design Studies on Less Rare-Earth and High Power Density Flux Switching Motors with Hybrid Excitation/Wound Field Excitation for HEV Drives,” Nagoya Institute of Technology, Japan, 2012.
- [129] W. Xu, J. Zhu, Y. Zhang, and J. Hu, “Cogging torque reduction for radially laminated flux-switching permanent magnet machine with 12/14 poles,” *IECON Proc. (Industrial Electron. Conf.)*, pp. 3590–3595, 2011.
- [130] M.-J. Jin, Y. Wang, J.-X. Shen, P. C.-K. Luk, W.-Z. Fei, and C.-F. Wang, “Cogging torque suppression in a permanent-magnet flux-switching integrated-starter-generator,” *IET Electr. Power Appl.*, vol. 4, no. December 2009, pp. 647–656, 2010.